Geological Quarterly, 2026, 70, 11
DOI: https://doi.org/10.7306/gq.1856

Geochemical and palaeontological insights into Middle Triassic Intra-Pontide ocean island fragments: Elmadağ Olistostrome, Central Anatolia

Kaan SAYIT[1, *], Cengiz OKUYUCU[2], U. Kagan TEKIN[3], Alaettin TUNCER[3] and Melikan AKBAŞ[4]

[1] Middle East Technical University, Department of Geological Engineering, 06800, Ankara, Türkiye;
ORCID: 0000-0001-6859-4536

[2] Ankara Hacı Bayram Veli University, School of Land Registry and Cadastre, 06500, Ankara, Türkiye;
ORCID: 0000-0002-5574-7852

[3] Hacettepe University, Department of Geological Engineering, 06800, Beytepe, Ankara, Türkiye;
ORCID: 0000-0001-5551-498X [U.K.T], 0000-0002-6623-3101 [A.T.]

[4] Konya Technical University, Department of Geological Engineering, 42250, Konya, Türkiye;
ORCID: 0000-0001-8144-8939

Sayit, K., Okuyucu, C., Tekin, U.K., Tuncer, A., Akbaş, M., 2026. Geochemical and palaeontological insights into Middle Triassic Intra-Pontide ocean island fragments: Elmadağ Olistostrome, Central Anatolia. Geological Quarterly, **70**, 11; https://doi.org/10.7306/gq.1856

The Late Cretaceous closure of the Neotethyan Intra-Pontide Ocean generated mélanges in front of southward-advancing nappes. These include the Elmadağ Olistostrome, which consists of blocks embedded in a Coniacian (Upper Cretaceous) siliciclastic to calcareous-siliciclastic matrix. This olistostrome locally contains basaltic blocks alternating with platform limestones. Benthic foraminifera from these limestones yielded Anisian ages in two localities east/southeast of Ankara (Central Anatolia). At the Taşönü locality, the Anisian to lower Ladinian basalt-limestone succession is overlain by an upper Ladinian sequence of volcanogenic clastic rocks, chert, and detrital limestone. At all localities, the basalts display alkaline compositions with typical OIB-like trace element signatures. High abundances of incompatible elements, coupled with high Nb/Zr, Zr/Y, and Nb/Y ratios, indicate a contribution from enriched/recycled components in their petrogenesis. Geological and geochemical evidence suggests that the basalt-limestone assemblage represents fragments of Anisian ocean islands in the Intra-Pontide Ocean. These islands were accreted to the southern Pontide margin during the late Ladinian. Following the closure of the Intra-Pontide Ocean during the Late Cretaceous, the Elmadağ Olistostrome was emplaced onto the Middle Triassic basement and the Jurassic-Cretaceous carbonate cover of the Sakarya Continent, as well as on the Izmir-Ankara-Erzincan ophiolitic mélange.

Key words: geochemistry, Neotethys, mantle plume, mélange, nappe, OIB.

INTRODUCTION

The Anatolian landmass is composed of several microcontinents (or terranes) whose final amalgamation occurred through the closure of Neotethys during the Alpine Orogeny (Şengör and Yılmaz, 1981; Göncüoğlu et al., 1997). Neotethys is a multi-branched oceanic entity, in which the Intra-Pontide and Izmir-Ankara-Erzincan (IAE) oceans (represented by their respective suture zones in Fig. 1) characterize the Northern Neotethyan oceanic domains. These two branches were previously thought to have opened during Liassic rifting (Şengör and Yılmaz, 1981). However, recent studies have shown that the IAE oceanic basin was already deep by the early Permian (Tekin et al., 2019), significantly earlier than previously thought, and that the Anisian (Middle Triassic) was marked by oceanic back-arc magmatism (Sayit et al., 2017). The other northern realm, the Intra-Pontide Ocean, was a deep basin by at least the latest Permian (Tekin et al., 2025). Therefore, it appears that these two domains were already open before the closure of Palaeotethys.

The Sakarya Zone (Okay, 1989) or Sakarya Composite Terrane (Göncüoglu et al., 1997) is a landmass comprising the Sakarya Continent of Şengör and Yılmaz (1981) as well as the Central and Eastern Pontides. The Sakarya Terrane is bordered by the Intra-Pontide Ocean to the north and the IAE Ocean to the south. This terrane contains a variably deformed and metamorphosed unit, called the Karakaya Complex, which stretches from NW to NE Türkiye (Şengör et al., 1984; Okay and Göncüoğlu et al. 2004). This unit has long been linked to the Palaeotethyan events due to its presumed pre-Lower Jurassic age. However, its relationship with Palaeotethys, an older Middle/Late Paleozoic-Early Mesozoic oceanic realm (e.g., Şengör, 1979; Stampfli and Borel, 2002), remains debated (for detailed information, the reader is referred to Okay

* Corresponding author; e-mail: ksayit@metu.edu.tr

Received: January 19, 2026; accepted: March 23, 2026; first published online: April 21, 2026

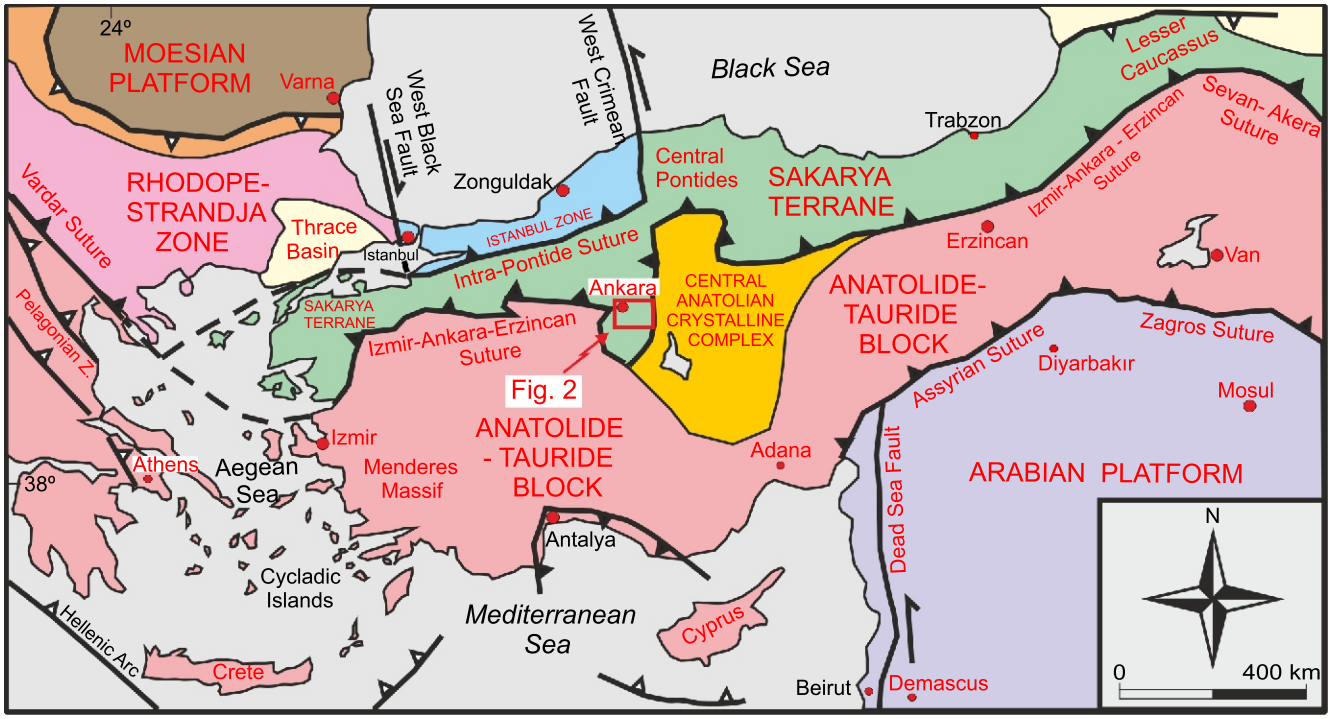

Fig. 1. Tectonic map of Türkiye and its surroundings with major suture zones and terranes, and the location of the study area east and south-east of Ankara city (slightly revised after Okay and Tüysüz, 1999; Okay and Göncüoğlu, 2004)

and Göncüoğlu, 2004; Sayit and Göncüoğlu, 2013). Within this context, this unit is viewed to represent either the continental back-arc basin of Palaeotethys (the Karakaya Marginal Sea of Şengör and Yılmaz, 1981) or Palaeotethys itself (e.g., Pickett and Robertson, 1996; Okay, 2000). A critical issue in these interpretations is that the Karakaya Complex is traditionally regarded as a pre-Liassic unit, due to the uppermost Triassic closure of Palaeotethys in the Anatolian region and the Karakaya Sea (Şengör and Yılmaz, 1981; Okay, 2000). This assumption is mainly based on the ages of the limestone blocks, which yielded ages no younger than Upper Triassic (e.g., Bingöl et al., 1975; Okay et al., 1990, 1991; Okay and Altıner, 2004), and that the Karakaya Complex is unconformably overlain by Liassic sedimentary rocks (Altıner et al., 1991). The inferred pre-Liassic age has served as a primary criterion for distinguishing the Karakaya Complex from the Neotethyan branches, whose closure is dated to Late Cretaceous-Paleocene (e.g., Şengör and Yılmaz, 1981; Göncüoğlu et al., 2000). In this regard, the recent finding of Tekin et al. (2025) challenges the previous interpretations. They showed that a major part of the Karakaya Complex, assumed to be the slightly metamorphic or non-metamorphic portion (the so-called Upper Karakaya Complex), is Cretaceous in age, rather than Triassic. Tekin et al. (2025) also reclassified the Upper Karakaya Complex as part of the Coniacian (Upper Cretaceous) Elmadağ Olistostrome (Erol, 1956; Tekin et al., 2024), a sedimentary mélange derived from the Intra-Pontide domain, rather than the Palaeotethys.

The discovery of an Upper Cretaceous age is crucial, as it challenges the classical view of the Karakaya Complex and its Palaeotethyan affinity, and necessitates a reassessment of the geodynamic evolution of the Sakarya Continent. In this study, we focus on a part of the Elmadağ Olistostrome in the Ankara region (Central Anatolia) that contains basalt-bearing blocks. These basalts, displaying OIB-type geochemistry (see also Sayit and Göncüoğlu, 2009; Sayit et al., 2010; Sayit, 2023), are primarily associated with Anisian (Middle Triassic) platform limestones and are overlain by an upper Ladinian (Middle Triassic) sedimentary sequence including spiculite/radiolarian cherts and detrital limestones. By combining whole-rock geochemistry with precise palaeontological ages extracted from the associated sedimentary rocks (from both platform limestones and spiculite/radiolarian cherts), we shed light on: i) the tectonic setting of the OIB-type basalts, ii) the geodynamics of the Intra-Pontide realm during the Middle Triassic, and iii) the mechanisms by which these basaltic masses were incorporated into the Elmadağ Olistostrome, and subsequently transported and emplaced onto the Sakarya Continent and accretionary deposits of the IAE Ocean.

GEOLOGICAL SETTING

The Ankara region contains a part of the Sakarya Zone (Okay, 1989) or Sakarya Composite Terrane (Göncüoğlu et al., 1997), which is delimited by two suture zones: the Intra-Pontide Suture Zone to the north and the Izmir-Ankara-Erzincan Suture Zone to the south (Fig. 1). The Ankara region hosts four major rock units (Fig. 2); i) The Dikmen Greywacke (Erol, 1956; Tekin et al., 2025), the oldest unit exposed in the region, mainly characterized by very low- to low-grade metaclastic rocks of Middle Permian to middle Upper Triassic age; ii) the Upper Cretaceous Elmadağ Olistostrome (Erol, 1956; Tekin et al., 2024), consisting of different types of blocks (platform/pelagic carbonates and cherts) within a clastic/carbonate matrix; iii) The Ankara Ophiolitic Mélange, chiefly made up of remnants of the IAE oceanic lithosphere (e.g., Rojay, 2013); and iv) Upper Cretaceous (Santonian) to Quaternary clastic, carbonate, and volcanic rocks.

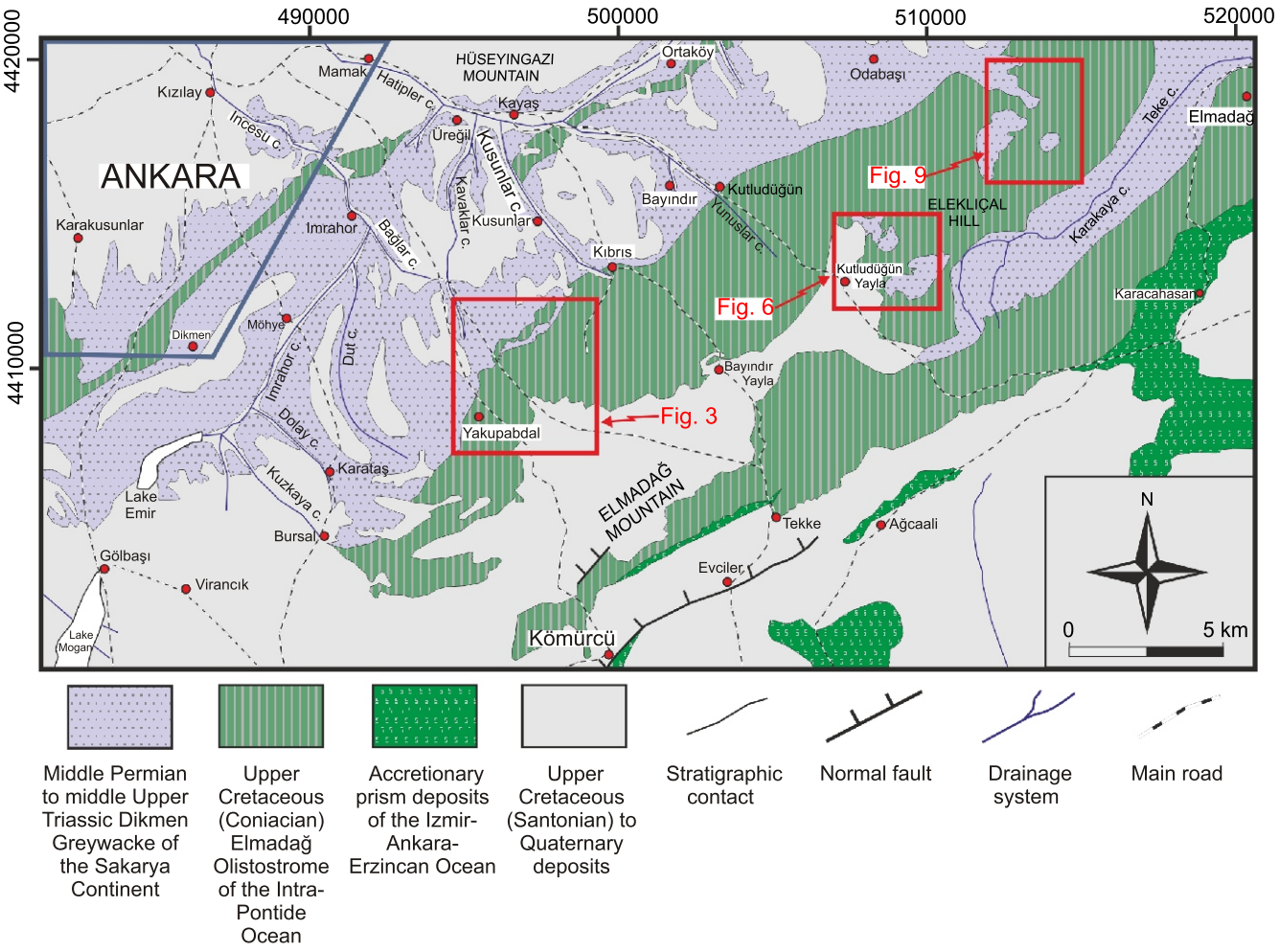

Fig. 2. Geological map of the east and southeast of the Ankara region (simplified and revised after Erol, 1956), showing the locations of study areas (indicated by red rectangles) at Yakupabdal (Fig. 3), Kutludüğün Yayla (Fig. 6) and Taşönü (Fig. 9)

GEOLOGICAL CHARACTERISTICS OF THE SECTIONS STUDIED

Samples for geochemical and palaeontological determinations were collected from three stratigraphic sections (Çayırlık, Zincancının-1, and Taşönü) on blocks within the Elmadağ Olistostrome (east/southeast Ankara, Central Anatolia; Fig. 2). Details of the stratigraphic sections from west to east are as follows.

ÇAYIRLIK SECTION

This stratigraphic section, located on the SE bank of Çayırlık creek in the Yakupabdal region (between coordinates 4411351N/498950E and 4411425N/499000E, UTM Zone 36S; Fig. 3) has a total thickness of 61 m and is named after the creek (Fig. 4). The section was measured on a single block within the Elmadağ Olistostrome. This block exceeds 200 m in thickness and is composed of alternating green to yellowish green altered basalt, and grey to beige medium- to thick-bedded platform limestone (Figs. 3–5). Five samples (Çay-1 to Çay-5) were collected from the section (Figs. 4 and 5); three samples (Çay-2, Çay-3, and Çay-4) were selected for benthic foraminifera determinations, while two samples (Çay-1 and Çay-5) were chosen for geochemical analysis (Figs. 4 and 5). In previous studies (Akyürek et al., 1984), an Anisian (Middle Triassic) age was assigned to this block based on its benthic foraminifera content.

ZINCANCININ-1 SECTION

The Zincancının-1 section, located in the eastern part of Kutludüğün Yayla on the SE bank of the Zincancının creek (between coordinates 4413069N/509623E and 4413093N/509632E, UTM Zone 36S), has a total thickness of 26 m (Figs. 6 and 7). The section was measured on a small block within the mélange and is composed of an alternation of green- to yellowish green-coloured altered pillow basalts and grey- to beige-coloured, very thick-bedded platform limestones (Fig. 8).

TAŞÖNÜ SECTION

The Taşönü section, located on the northern bank of the Taşönü creek (between coordinates 4419017N/513414E and 4419000N/513323E, UTM Zone 36S), was measured on a block within the Elmadağ Olistostrome (Figs. 9 and 10) and has a total thickness of 88.3 m. The basal part of the section consists of green to yellow altered pillow basalts with intra-pillow platform limestone lenses (Figs. 10 and 11A–C). This is followed by alternating green to yellow thin-bedded volcaniclastic sandstone and mudstone with platform limestone lenses (Fig. 11D). Higher in the section, green to yellow altered pillow basalts with intra-pillow platform limestone lenses form the dominant lithology (Fig. 11E, F). This part is followed by volcanogenic conglomerate with limestone clasts. This is overlain by thick (~40 cm) grey to beige thin- to medium-bedded

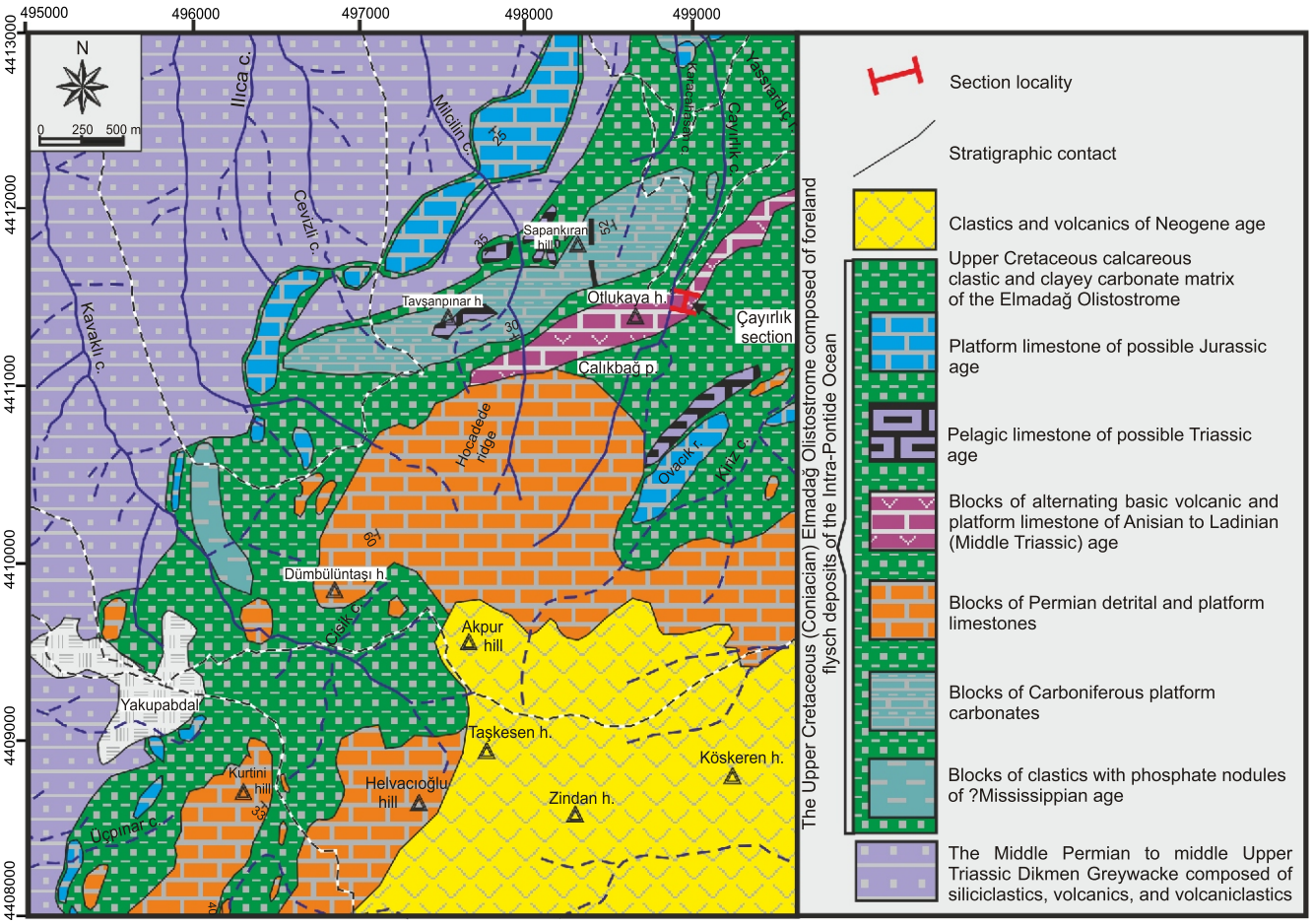

Fig. 3. Geological map of the Yakupabdal area and its surroundings, showing the location of the Çayırlık stratigraphic section (slightly revised after Tekin and Tuncer, 2024)

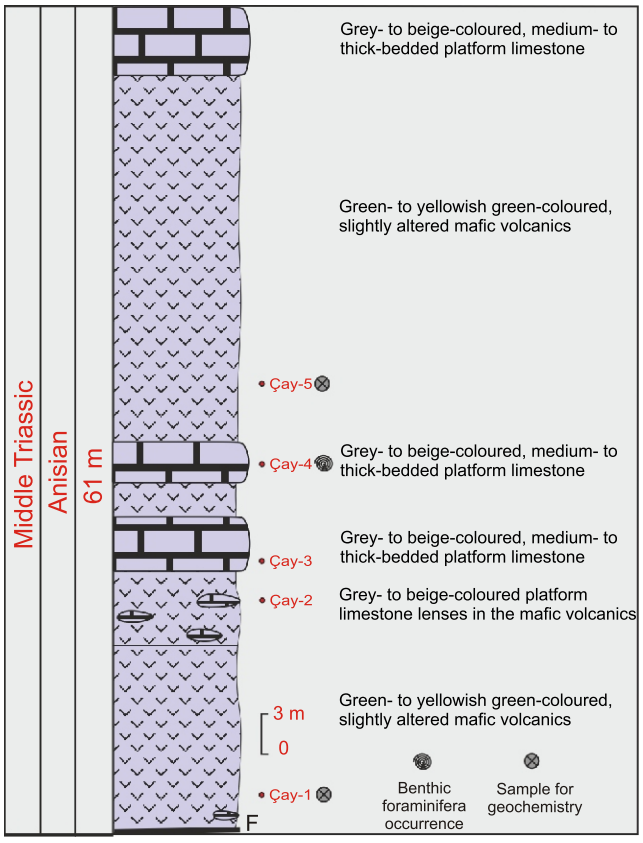

platform limestone lenses (Fig. 11G, H). The upper part of the section (~6.7 m) is made up of alternating green thin-bedded spiculite/radiolarian chert, mudstone, and grey detrital limestone (Fig. 11I–K). The uppermost part of the section is represented by alternating green to yellow thin-bedded volcanogenic sandstone and mudstone (Fig. 11L).

Among the basalt samples collected from the section, four (Taş-4, Taş-5, Taş-6, and Taş-13) were suitable for geochemical analysis. Benthic foraminifera were obtained from three samples (Taş-8, Taş-17, and Taş-25). Several samples were collected from overlying chert layers, but only one (Taş-21) was suitable for radiolarian analysis.

Fig. 4. Log of the Çayırlık section and sampling levels

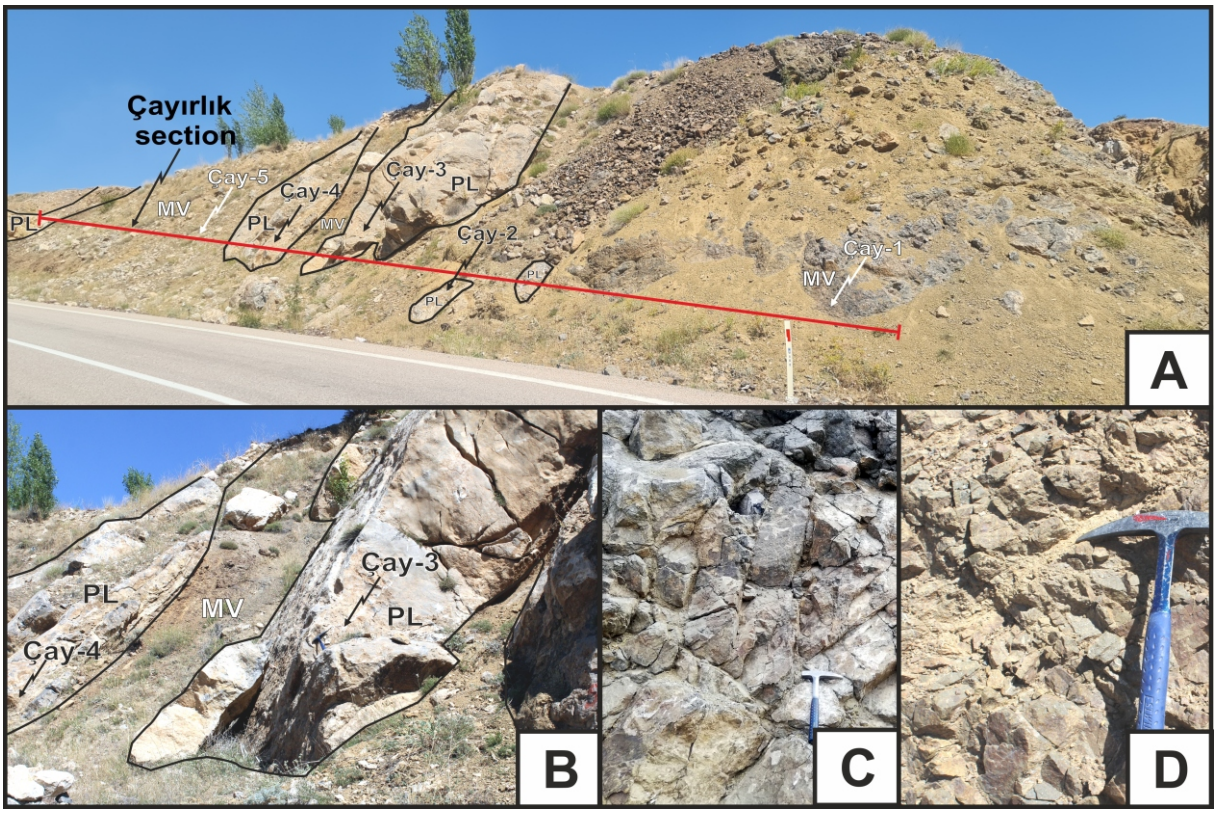

Fig. 5. Field photographs from the Çayırlık section, showing the sampled block within the Elmadağ Olistostrome in the Yakupabdal region

A – general view of the Çayırlık section showing the relations between mafic volcanic rocks and platform limestones, along with sampling points; **B** – the contact between mafic volcanic rocks and platform limestones in the central part of the section, where samples Çay-3 and Çay-4 were collected; **C –** detailed view of the grey to beige thick-bedded platform limestone from which sample Çay-3 was retrieved; **D** – mafic volcanic rocks in the upper part of the section where the sample Çay-5 was taken; abbreviations: MV – mafic volcanic rocks, PL – platform limestone

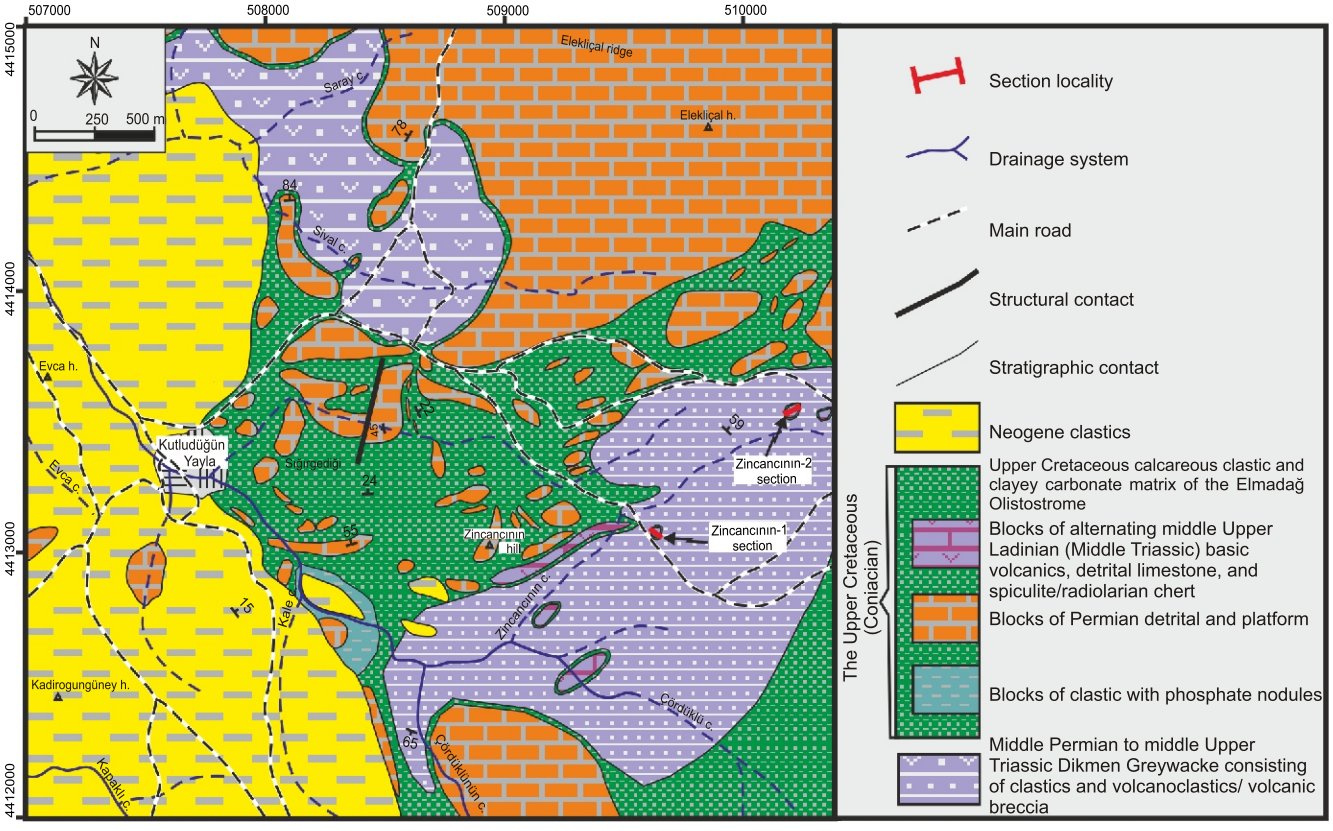

Fig. 6. Geological map of the Kutludüğün Yayla region, showing the locations of Zincancının-1 and Zincancının-2 (corresponding to the Zincancının section in Tekin et al., 2025) stratigraphic sections (slightly revised after Tekin and Tuncer, 2024)

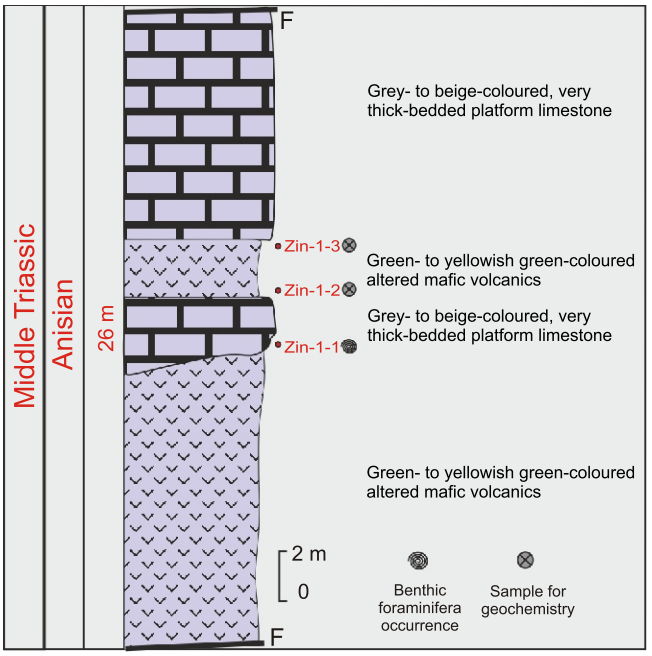

Fig. 7. Log of the Zincancının-1 section and sampling levels

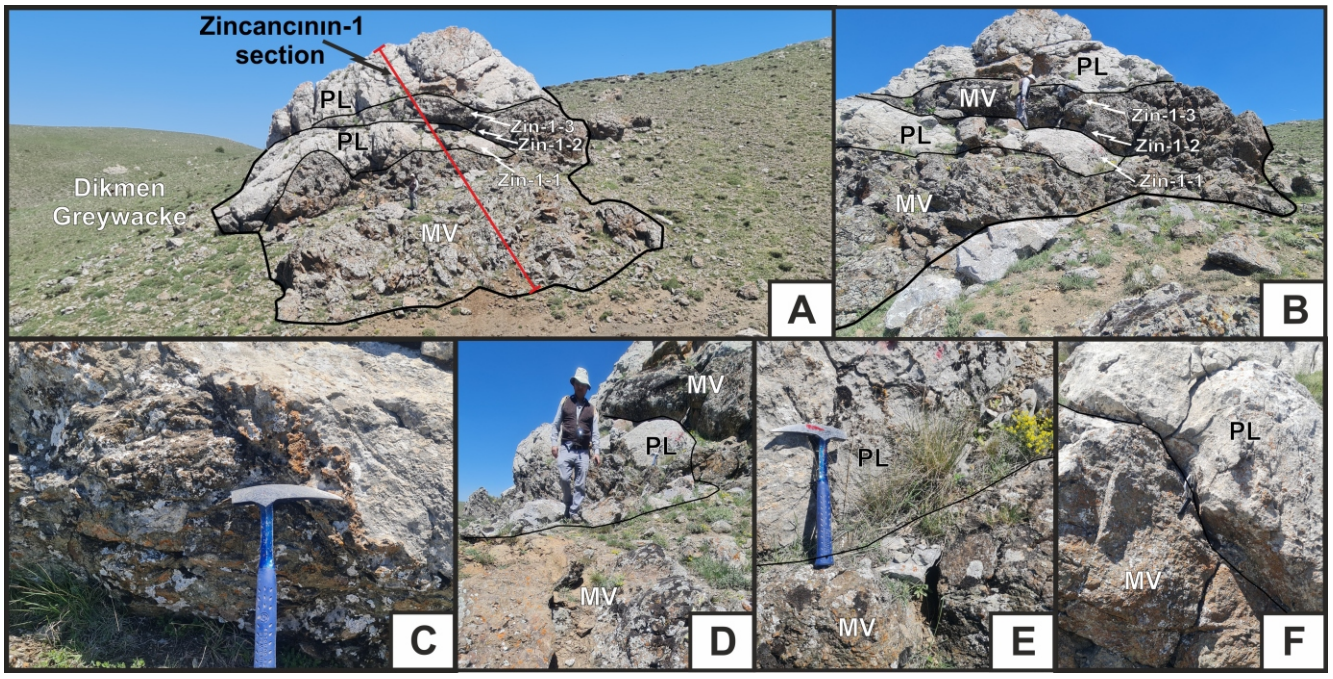

Fig. 8. Field photographs of the Zincancının-1 section, measured along a block within the Elmadağ Olistostrome

A – general view of the section, showing the block in olistostrome overlying the Dikmen Greywacke; **B –** side view of the same block, illustrating the relationship between green to yellowish green altered mafic volcanic rocks and grey to beige very thick-bedded platform limestone; **C** – detailed view of the mafic volcanic rocks; **D –** view of the basal mafic volcanic rocks and platform limestone; **E** – detailed view from the central part of the section, showing the relation between mafic volcanic rocks and platform limestone; **F** – view from the uppermost part of the section, highlighting the relationship between mafic volcanic rocks and very thick platform limestone; other explanations as in Figure 5

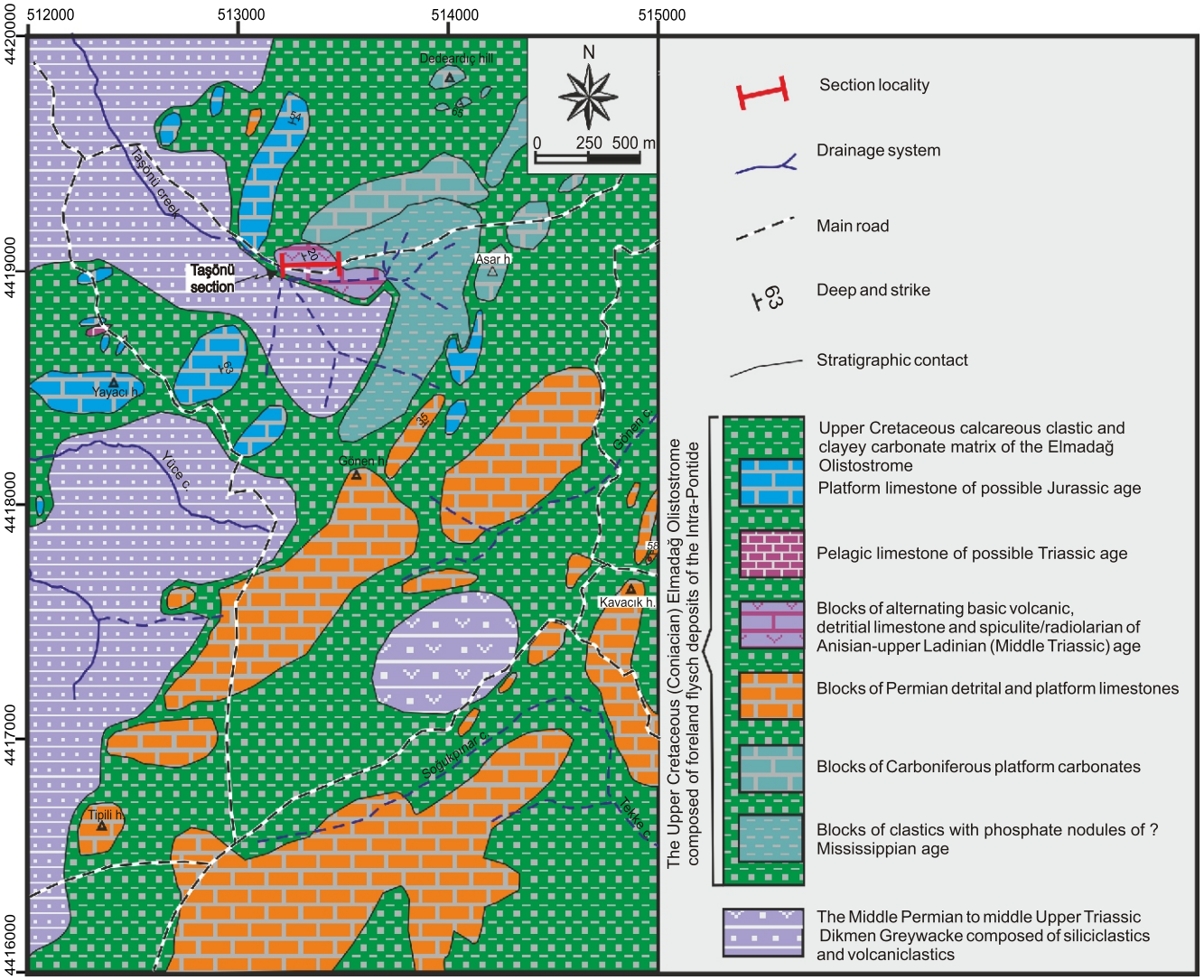

Fig. 9. Geological map of the vicinity of Taşönü, showing the location of the Taşönü stratigraphic section (slightly revised after Tekin and Tuncer, 2024)

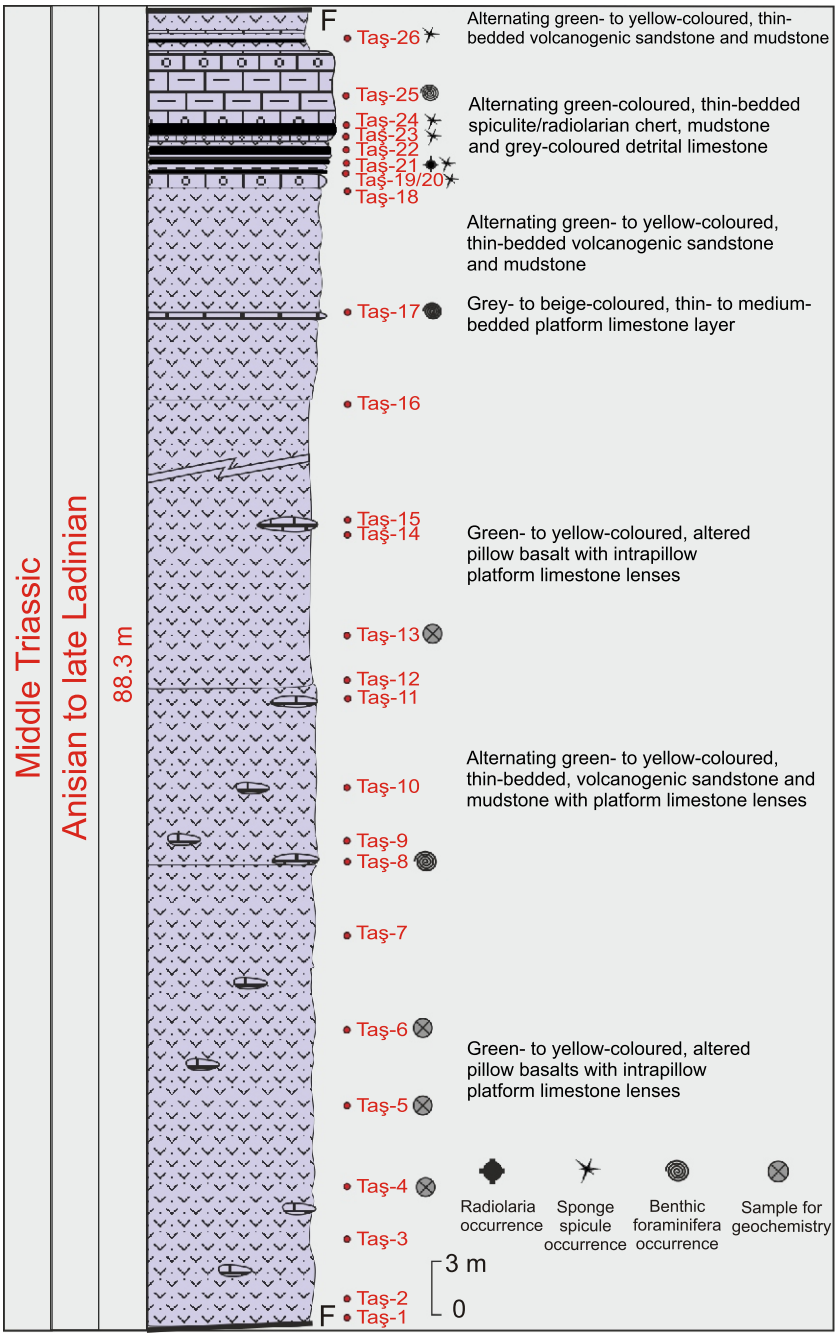

Fig. 10. Log of the Taşönü section and sampling levels

BIOCHRONOLOGY OF THE BENTHIC FORAMINIFERA AND RADIOLARIAN ASSEMBLAGES

BENTHIC FORAMINIFERA ASSEMBLAGE OF THE ÇAYIRLIK SECTION

From the Çayırlık section, three samples (Çay-2, Çay-3, and Çay-4) were collected to examine foraminiferal assemblage from the limestone beds interlayered with the mafic volcanic rocks (Fig. 4). Two samples, Çay-2 and Çay-3, proved barren. However, sample Çay-4 taken from a three-metre-thick carbonate level is rich in benthic foraminifera (*Endotriadella wirzi* (Koehn-Zaninetti), *Endotriada tyrrhenica* Vachard et al., *Diplotremina* sp. 1, and *Diplotremina* sp. 2, which enabled age assignment (Fig. 12).

Endotriadella wirzi, a characteristic taxon, is a typical Triassic species. Its first occurrence datum was reported by Rettori (1995) as Aegean (lower Anisian), and it is widely known worldwide in Lower-Middle Triassic strata, corroborated by conodont ages (e.g., Mietto et al., 1991). This species was first described by Koehn-Zaninetti (1969) from the upper Anisian strata in Almtal, Austria. Subsequently, it has been reported from middle-upper Anisian strata in the Carpathian Mountains (Salaj et

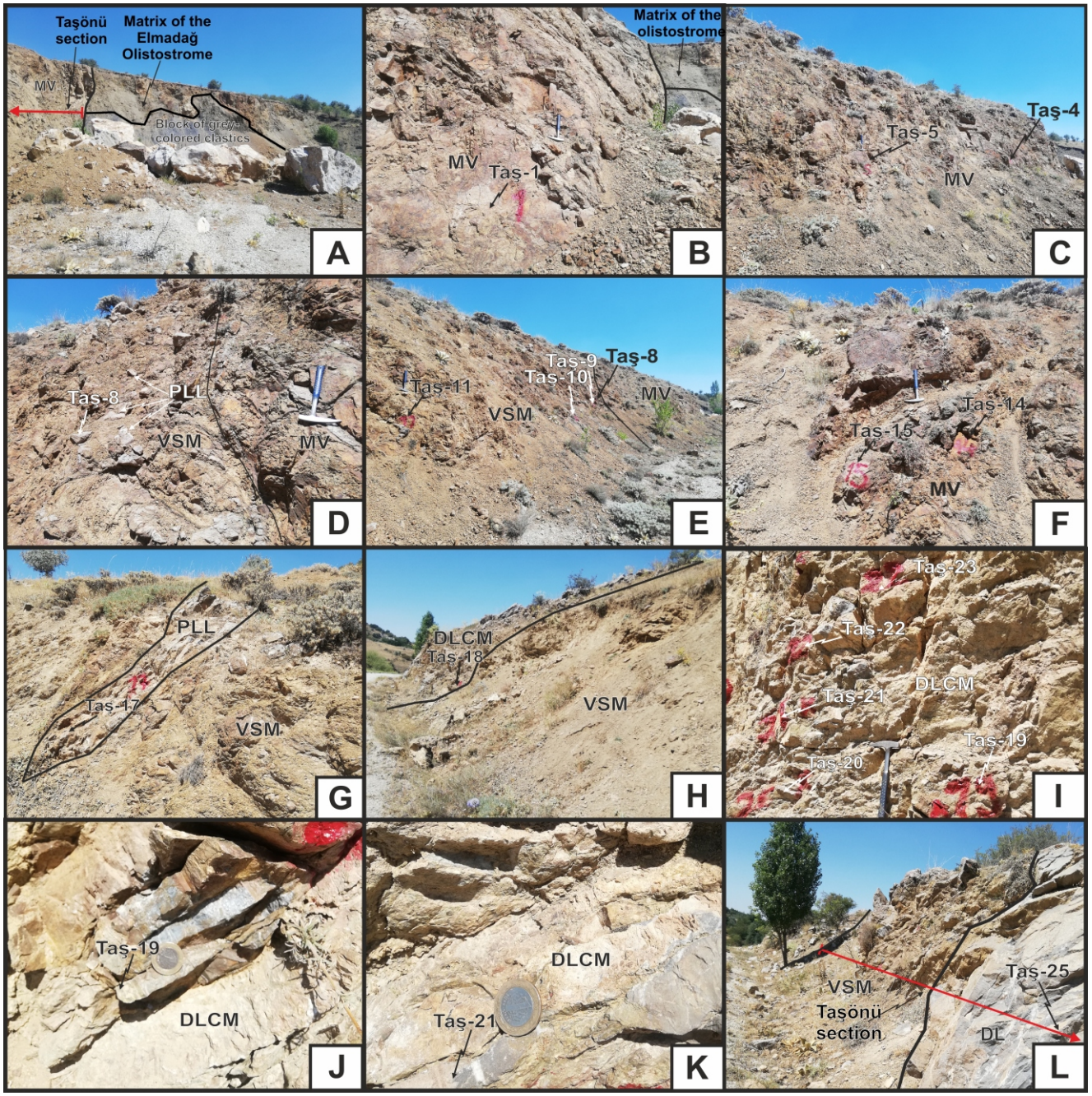

Fig. 11. Field photographs from the Taşönü section measured along a block within the Elmadağ Olistostrome

A, B – view from the basal part of the section, showing the matrix of the olistostrome with a possible Lower Carboniferous grey-coloured clastic block and block of mafic volcanic rocks forming the basal part of the Taşönü section; **C** – general view of the green to yellow pillow basalts with intrapillow limestones at the base of the section; **D** – view of the alternating green to yellow, thin- to medium-bedded sandstones and mudstones with platform limestone lenses where sample Taş-8 was collected; **E, F** – general view of the green- to yellow-coloured pillow basalts and platform intrapillow limestones in the central part of the section; **G** – grey to beige thin- to medium-bedded platform limestone lens (sample Taş-17) of Anisian to Carnian age, overlying green to yellow volcanogenic conglomerate; **H** – view from the upper part of the section, showing the boundary between underlying green to yellow thin-bedded sandstone and mudstone and overlying alternating green thin-bedded chert, mudstone, and grey detrital limestone; **I** – detailed view of the alternating chert, mudstone and detrital limestone corresponding to the interval between sample Taş-19 to Taş-24; **J** – detailed view of the alternating chert, mudstone and detrital limestone where sample Taş-19 was collected from the chert layer; **K** – detailed view from the alternating chert, mudstone and detrital limestone where sample Taş-21 was collected from a spiculite/radiolarian chert layer, indicating an upper Ladinian age; **L** – view from the uppermost part of the section, showing alternating green to yellow thin-bedded sandstone and mudstone overlying the grey to beige thick-bedded detrital limestone where sample Taş-26 was collected; abbreviations: MV – mafic volcanic rocks, VSM – alternating volcanogenic sandstone and mudstone, PLL – platform limestone lens, DLCM – alternating detrital limestone, chert and mudstone, DL – detrital limestone

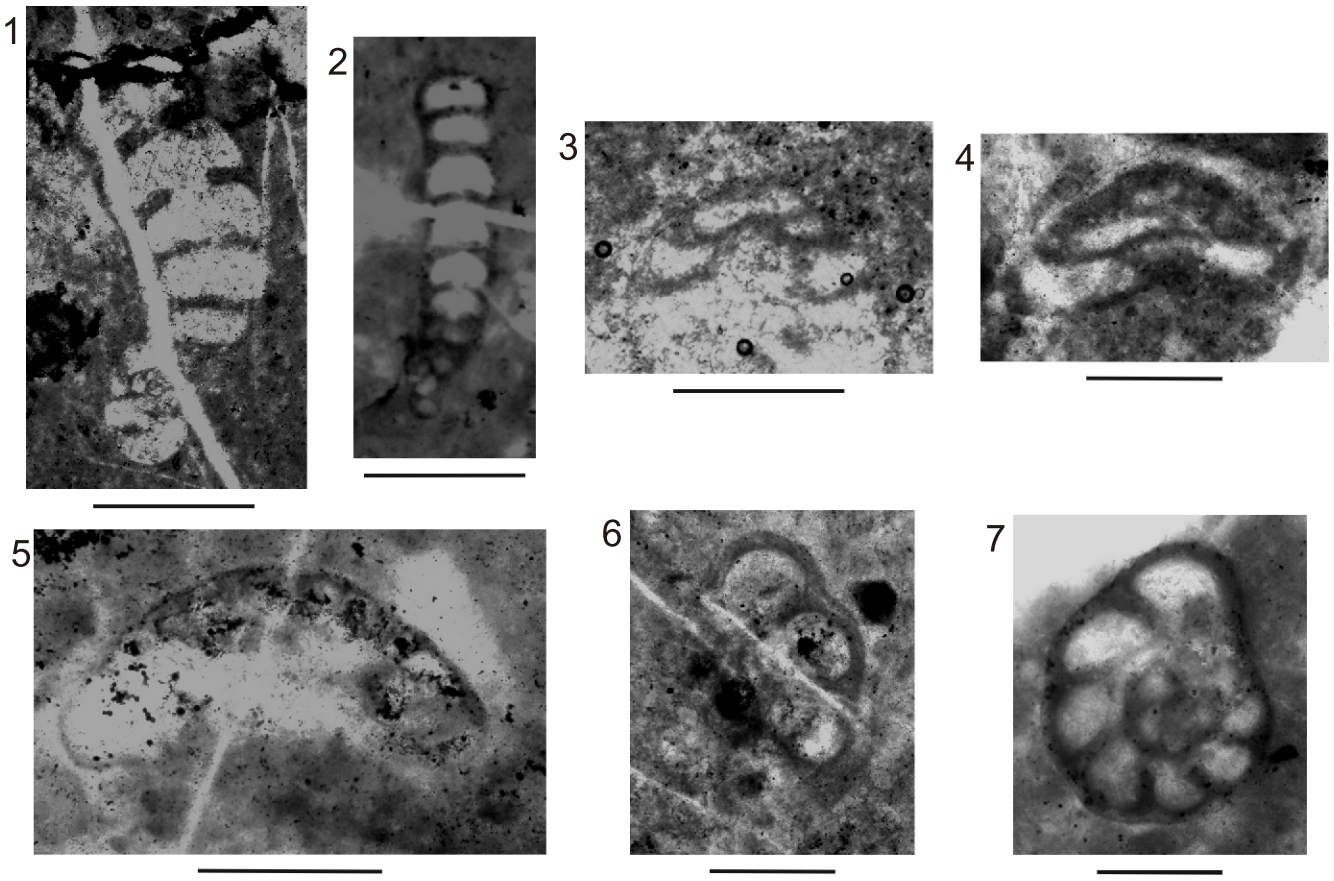

Fig. 12. Foraminifera of Anisian age from sample Çay-4 in the Çayırlık section

1, **2** – *Endotriadella wirzi* (Koehn-Zaninetti); **3**, **4** – *Diplotremina* sp. 1; **5** – *Diplotremina* sp. 2; **6**, **7** – *Endotriada tyrrhenica* Vachard et al.; Scale bar for 1, 2 is 0.5 mm and for 3–7 is 0.25 mm

al., 1983), from uppermost Pelsonian strata in Bulgaria (Trifonova and Ivanova, 2001), from uppermost Spathian (Olenekian)-lowermost Cordovelian (lowermost Carnian) strata in South China (Lehrmann et al., 2015; Song et al., 2015; Altıner et al., 2021), from Pelsonian (Anisian) beds in central Vietnam (Ueno et al., 2019), from Illyrian (upper Anisian) strata in Upper Silesia, Poland (Bucur and Matysik, 2020), from lower Anisian to lower Middle Anisian strata in Hungary (Hips, 2022), and middle-upper Anisian strata in Slovenia (Gale et al., 2023).

The upper Anisian-lower Norian occurrence of *Endotriada tyrrhenica* Vachard et al., another important taxon in the assemblage of sample Çay-4, was first described by Vachard et al. (1994). It has been reported from Upper Triassic strata in Slovenia (Gale et al., 2012), Türkiye (Beccaletto et al., 2005), northern Thailand (Miyahigashi et al., 2012; Ueno et al., 2012), and Japan (Chablais et al., 2010; see brief discussion in Altıner et al., 2021); it is common in Anisian strata in Italy (Emmerich et al., 2005), southern China (Lehrmann et al., 2015; Altıner et al., 2021), and Vietnam (Ha et al., 2019; Ueno et al., 2019). In sample Çay-4, undetermined specimens of the genus *Diplotremina* (*Diplotremina* sp. 1 and *Diplotremina* sp. 2) were previously reported from Middle-Upper Triassic strata by Zaninetti (1976). The genus *Diplotremina* has been described from Aegean (lower Anisian) beds in Japan (Kobayashi, 2008), from Norian-Rhaetian beds in Slovenia (Gale et al., 2011), from Pelsonian (Anisian) deposits in Vietnam (Ueno et al., 2019), and from uppermost Spathian (Olenekian)-Longobardian (Ladinian) strata in South China (Altıner et al., 2021). The evaluation of these taxa present in Çay-4 encompasses a relatively long stratigraphic range (Middle-Upper Triassic), but they are probably Anisian in age (Figs. 4 and 12).

BENTHIC FORAMINIFERA ASSEMBLAGE OF THE ZINCANCININ-1 SECTION

Sample Zin-1-1 from the Zincancının-1 section (Fig. 7) contains a diverse benthic foraminifera assemblage, including *Krikoumbilica pileiformis* He, *Endotriadella wirzi* (Koehn-Zaninetti), *Endoteba badouxi* (Zaninetti et al.), *Gaudryina* ex gr. *triadica* Kristan-Tollmann, *Polarisella* sp., *Endotriada* sp. and *Lamelliconus*? sp. (Fig. 13). Except for some long-ranging small foraminifers (e.g., *Polarisella* sp. and *Endotriada* sp.), some of the stratigraphically important taxa (e.g., *Krikoumbilica pileiformis, Endotriadella wirzi, Endoteba badouxi* and *Gaudryina* ex gr. *triadica*) in this sample are crucial for the age assignment.

The age-diagnostic taxon, *Krikoumbilica pileiformis,* was originally described from Anisian-Ladinian strata in Guizhou, southern China by He (1984). It has been subsequently reported from strata of the same age in western Australia (Apthorpe, 2003), Northern Italy (Emmerich et al., 2005), and southern China (Lehrmann et al., 2015; Altıner et al., 2021).

A typical Triassic species, *Endotriadella wirzi,* was first described by Koehn-Zaninetti (1969) from upper Anisian strata of Almtal, Austria. It has been subsequently reported from uppermost Spatian (Olenekian) to lowermost Cordovelian (Carnian)

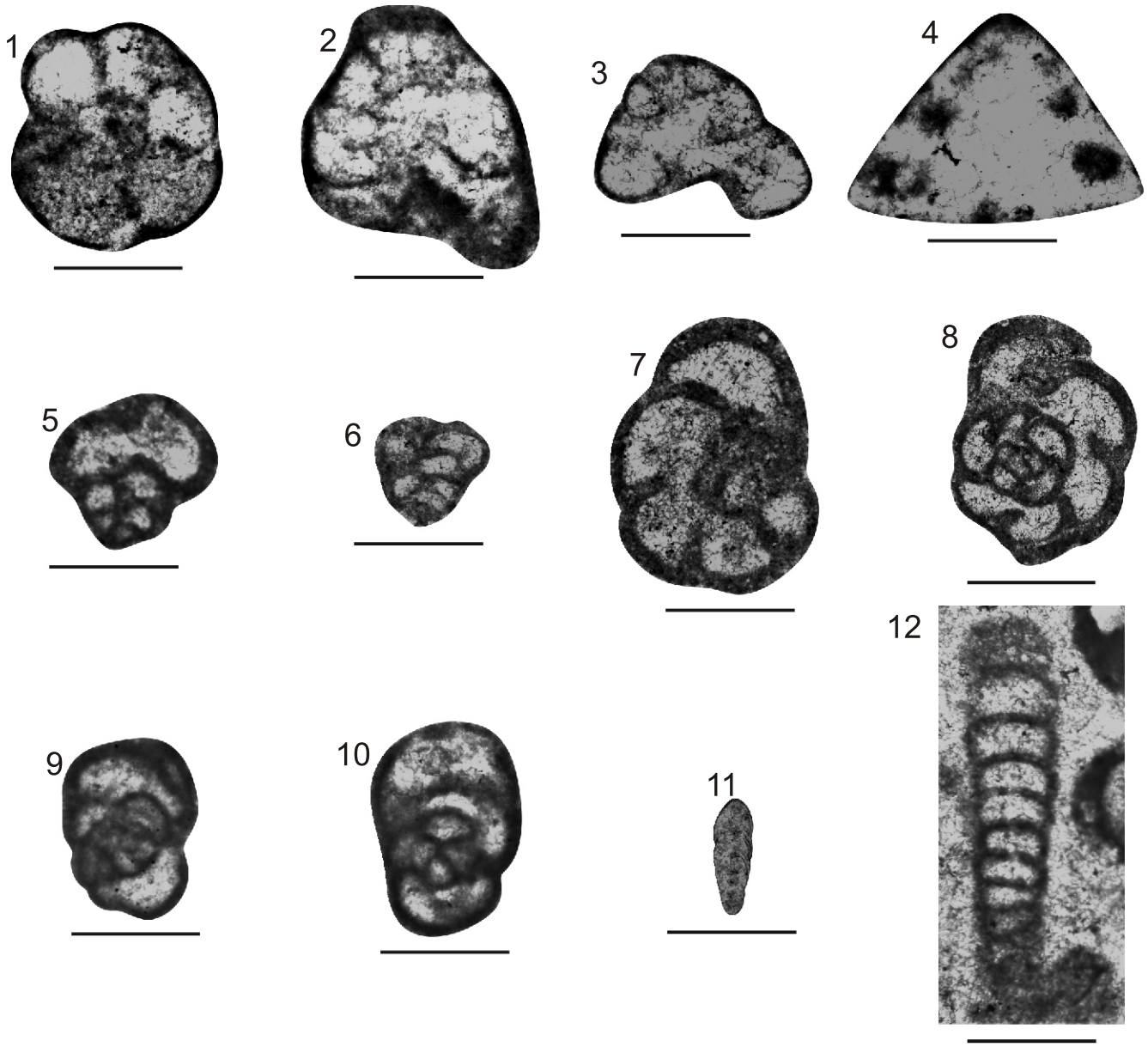

Fig. 13. Foraminifera of Anisian age from sample Zin-1-1 from the Zincancının-1 section

`**1–3** – *Krikoumbilica pileiformis* He; **4** – *Lamelliconus* ? sp.; **5, 6** – *Gaudryina* ex gr. *triadica* Kristan-Tollmann; **7, 8 –** *Endoteba badouxi* (Zaninetti et al.); **9, 10 –** *Endotriada* sp.; **11** – *Polarisella* sp.; **12** – *Endotriadella wirzi* (Koehn-Zaninetti); scale bar is 0.25 mm for all specimens

strata in different places within the Tethyan realm (e.g., Salaj et al., 1983; Trifonova and Ivanova, 2001; Lehrmann et al., 2015; Altıner et al., 2021; Gale et al., 2023).

Endoteba badouxi, another taxon identified in this sample, was first described from the upper Anisian strata of Switzerland by Zaninetti et al. (1972). Its range is Anisian to Carnian based on studies in various parts of the Tethyan realm (e.g., He and Wang, 1990; Rettori, 1995; Emmerich et al., 2005; Velledits et al., 2011; Altıner et al., 2021). The other important Triassic taxon, *Gaudryina* ex gr. *triadica* Kristan-Tollmann, has been reported from Spathian strata in southern China (Song et al., 2011), from Anisian to Carnian-Rhaetian beds in Japan (Kobayashi, 1996; Kobayashi et al., 2005; Chablais et al., 2010; Peyrotty et al., 2020), and from Carnian beds in Thailand (Kobayashi et al., 2006; Miyahigashi et al., 2012).

The genus *Polarisella* is a long-ranging taxon in this sample, and its range was from Cisuralian to Anisian (Middle Triassic; Gaillot and Vachard, 2007). It may range into the Jurassic, based on studies in Germany (Gaillot and Vachard, 2007; Vachard, 2016). *Endotriada* sp. is another long-ranging taxon in sample Zin-1-1, and has been described from Anisian to Rhaetian strata in previous studies (e.g., Vachard et al., 1994; Kobayashi, 2008; Gale et al., 2012; Altıner et al., 2021). Taking into consideration the first and last occurrences of the taxa determined in sample Zin-1-1, the age represented is most probably Anisian (Fig. 7).

BENTHIC FORAMINIFERA AND RADIOLARIAN ASSEMBLAGES OF THE TAŞÖNÜ SECTION

BENTHIC FORAMINIFERA ASSEMBLAGE OF THE TAŞÖNÜ SECTION

Foraminiferal assemblages were obtained from three samples (Taş-8, Taş-17 and Taş-25) from the Taşönü section. Two samples (Taş-8 and Taş-17) were obtained from platform limestone lenses, and one (Taş-25) was retrieved from a detrital limestone layer located in the upper part of the section (Fig. 10).

Sample Taş-8 was retrieved from a small, lens-shaped platform limestone within interbedded green to yellow, thin-bedded volcaniclastic sandstones and mudstones (Fig. 10). This sample includes a very characteristic foraminiferal taxon, *Meandrospira dinarica* Kochansky-Devidé and Pantič (Fig. 14A), an important species in Anisian strata, especially in the Tethyan Belt, that first appears at the base of the Anisian based on previous studies (e.g., Rettori, 1995; Altıner et al., 2021). It has also been reported from Anisian strata in the southern Carpathians (Bucur et al., 1994), in Japan (Kobayashi, 1996; Kobayashi et al., 2005), Vietnam (Martini et al., 1998), northern Italy (Fugagnoli and Posenato, 2004; Berra et al., 2005), Hungary (Velledits et al., 2011), southern China (Altıner et al., 2021) and Croatia (Kukoč et al., 2023).

Sample Taş-17 was collected from a green to beige, thin- to medium-bedded platform limestone lens within the interbedded green to yellow, thin-bedded volcaniclastic sandstones and mudstones (Fig. 10). Only *Turriglomina mesotriasica* (Koehn-Zaninetti) was recovered from this sample (Fig. 14); it has been reported from Triassic strata within the different parts of the Tethyan realm (Zaninetti, 1976; Rettori, 1995). The range of this species is Anisian to Carnian according to previous studies (e.g., Rettori et al., 1994; Bucur et al., 1994; Emmerich et al., 2005; Bedi et al., 2013; Altıner et al., 2021).

Sample Taş-25 was taken from a detrital limestone in the upper part of the Taşönü section (Fig. 10), a part of the section mainly represented by alternating green, thin-bedded chert-mudstone and grey detrital limestone (Fig. 10). Together with some long-ranging foraminiferan species, calcareous algae, cyanobacteria, and microproblematica (e.g., *Tauridiopsis* sp., *Bisphaera* sp., *Mizzia* sp., *Girvanella* sp., and *Tubiphytes* sp.), this sample includes many age-diagnostic taxa.

The faunal and floral assemblages of this detrital limestone include relatively diverse assemblages from different stratigraphic levels, including *Kalijanella karpinensis* Petrova, *Langella conica* Sellier de Civrieux and Dessauvagie, *L. perforata* (Lange), *Geinitzina* ex gr. *postcarbonica* Spandel, *Langella* sp., *Robuloides* sp., *Uralogordiopsis*? sp., *Bisphaera* sp., *Tauridiopsis* sp., *Archaediscus* sp., *Mizzia* sp., *Girvanella* sp., *Koninckopora* sp., *Tubiphytes* sp. (microproblematica; Fig. 14).

Kalijanella karpinensis, represented by a typical specimen in terms of morphology and wall structure, was first described by Petrova (1981) from the Middle Devonian succession in the central and northern Urals. Two *Langella* taxa (*Langella conica* and *L. perforata*) are other important taxa recovered from this sample, and they have been widely described from the Middle to Upper Permian strata of different parts of the Tethyan realm (e.g., Leven and Okay, 1996; Ünal et al., 2003; Hamdi et al., 2009; Şahin et al., 2012; Nejad et al., 2015).

Geinitzina ex gr. *postcarbonica* is among the long-ranging taxa, having been recorded throughout the entire Permian succession (e.g., central America by Spandel, 1901; Groves and Boardman, 1999; Iran by Bozorgnia, 1973; southern China by Wang, 1982; Japan by Ueno, 1989; Mexico by Vachard et al., 1993; Bolivia by Mamet, 1996; Türkiye by Ünal et al., 2003 and Tekin et al., 2019). Although not identifiable to species level due to insufficient material, the genus *Robuloides* in the assemblage has been previously reported from Capitanian to uppermost Changhsingian strata in Greece, Cyprus, Hungary, Türkiye, Iran, NW Caucasus, southern China, Japan, and New Zealand (e.g., Gaillot and Vachard, 2007; Nejad et al., 2015).

Koninckopora, an important calcareous alga with worldwide distribution found in this sample, is known from middle to upper Viséan strata (MFZ11 to MFZ15 biozones; Vachard et al., 2014). Recent studies (e.g., Mamet, 1991; Cózar et al., 2008; Groves et al., 2012; Vachard et al., 2016) have also recorded it from lower Serpukhovian strata. The genus *Archaediscus* is a long-ranging taxon and has been reported from middle Viséan to lowermost Moscovian strata (e.g., Pille, 2008; Kobayashi and Vachard, 2022; Cózar et al., 2023).

The youngest age inferred from this sample is the uppermost Changhsingian, hence the depositional age of this sample can be interpreted as the uppermost Changhsingian or younger (Fig. 10). Based on the radiolarian assemblage of the sample derived from the underlying level (sample Taş-21), the upper part of this section can be dated as upper Ladinian (Fig. 10).

RADIOLARIAN ASSEMBLAGE OF THE TAŞÖNÜ SECTION

Although seven samples (Taş-19 to Taş-24 and Taş-26) were collected from spiculite/radiolarian chert layers from the upper part of the Taşönü section, they are mainly rich in sponge spicules (Fig. 10) and only one sample (Taş-21) includes less-diverse and moderately-preserved radiolarians (Fig. 15). Based on the presence of very rich sponge spicules and rare radiolarian assemblages, it can be inferred that sedimentation of this part of the section took place in shallow sea conditions with circulation from the open sea and rich in SiO_2 saturation related to the volcanic activities (De Wever et al., 2001; Flügel, 2004).

Five radiolarian taxa from the Entactinaria (*Muelleritortis cochleata cochleata* (Nakaseko and Nishimura), *M. expansa* Kozur and Mostler, *Tritortis kretaensis dispiralis* (Bragin), *Pseudostylosphaera* sp. cf. *P. canaliculata* (Bragin), *P. imperspicua* (Bragin) were determined from sample Taş-21 from the Taşönü section (Fig. 15). Three important taxa (*Pseudostylosphaera imperspicua, Muelleritortis cochleata cochleata* and *M. expansa*) first appear at the base of the upper Ladinian (base of the Longobardian corresponding to the base of *Pterospongus priscus* Subzone of the *Muelleritortis cochleata* Zone) based on previous studies (e.g., Nakaseko and Nishimura, 1979; Kozur, 1988; Bragin, 1991; Kozur and Mostler, 1994; Sugiyama, 1997; Tekin, 1999; Gorican et al., 2005; Tekin and Göncüoğlu, 2007; Tekin and Sönmez, 2010; Bragin et al., 2016; Fig. 16). While the LAD of *Pseudostylosphaera imperspicua* is at the top of the *Spongoserrula fluegeli* Subzone of the *Muelleritortis cochleata* Zone based on the zonal scheme by Kozur and Mostler (1994, 1996) and Kozur (2003) in the upper Ladinian, two of the taxa (*Muelleritortis cochleata cochleata* and *M. expansa*) last appear in the basal part of the lower Carnian.

On the other hand, the FAD of the *Tritortis kretaensis dispiralis* is at the base of the *Spongoserrula fluegeli* Subzone of the *Muelleritortis cochleata* Zone, whereas it last appears at the base of the lower Carnian based on previous studies (e.g., Bragin, 1991; Cordey et al., 1988; Kozur, 1988; Dosztaly, 1989; Kozur and Mostler, 1996; Kametaka et al., 1997; Tekin, 1999; Hauser et al., 2001; Tekin and Göncüoğlu, 2007). Based on the co-occurrence of *Pseudostylosphaera imperspicua* and *Tritortis kretaensis dispiralis* in sample Taş-21, the age of this sample is upper Upper Ladinian (upper Longobardian) corresponding to the *Spongoserrula fluegeli* Subzone of the *Muelleritortis cochleata* Zone based on the zonal scheme by Kozur and Mostler (1994, 1996) and Kozur (2003).

According to the previous study (Tekin et al., 2025), a roughly coeval radiolarian assemblage including *Baumgartneria curvispina* Dumitrica, *Pterospongus* sp., *Sarla* sp., *Spongoxystris*? sp. cf. *S.* cf. *slovenica* (Kolar-Jurkovsek), *Pseudostylosphaera gracilis* Kozur and Mock, *P. inaequata* (Bragin), *P. multispinata* Tekin and Mostler, *P. nazarovi* (Kozur and Mostler) and *Muelleritortis cochleata koeveskalensis* Kozur was obtained from the Zincancının-2 section (marked as the

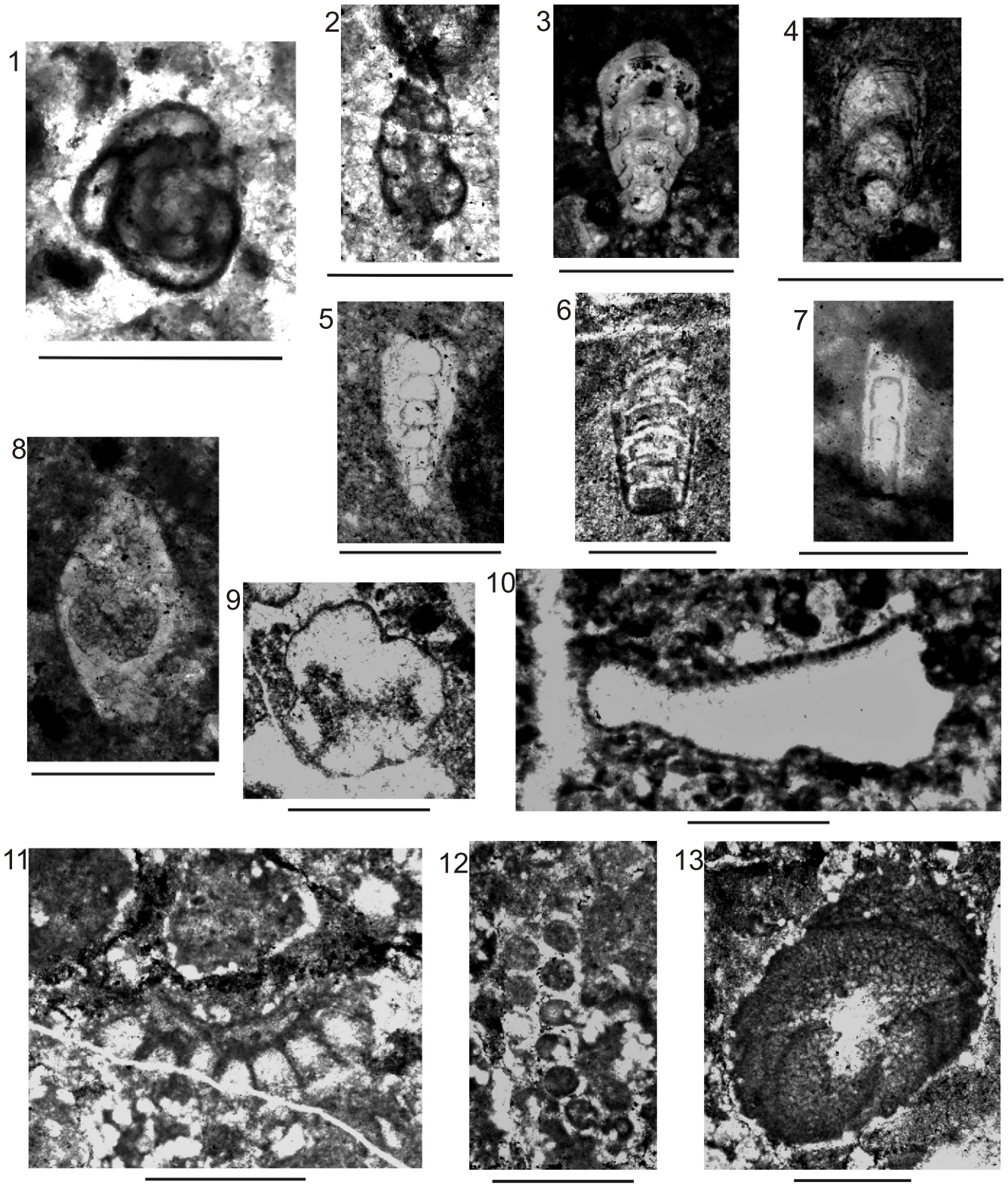

Fig. 14. Foraminifera of Anisian to Ladinian age from samples Taş-08, Taş-17, and Taş-25 in the Taşönü section

1 – *Meandrospira dinarica* Kochansky-Devidé and Pantić, Taş-08; **2** – *Turriglomina mesotriasica* (Koehn-Zaninetti), Taş-17; **3** – *Langella conica* Sellier de Civrieux and Dessauvagie, Taş-25; **4** – *Langella perforata* (Lange), Taş-25; **5** – *Langella* sp., Taş-25; **6** – *Geinitzina* ex gr. *postcarbonica* Spandel, Taş-25; **7** – *Tauridiopsis* sp., Taş-25; **8** – *Robuloides* sp., Taş-25; **9** – *Bisphaera* sp., Taş-25; **10** – *Kalijanella karpinensis* Petrova, Taş-25; **11** – *Koninckopora* sp., Taş-25; **12** – *Mizzia* sp., Taş-25; **13** – *Tubiphytes* sp., Taş-25; scale bar for figures 1, 2 and 5–8 is 0.25 mm, and for figures 3, 4 and 9–13 is 0.5 mm

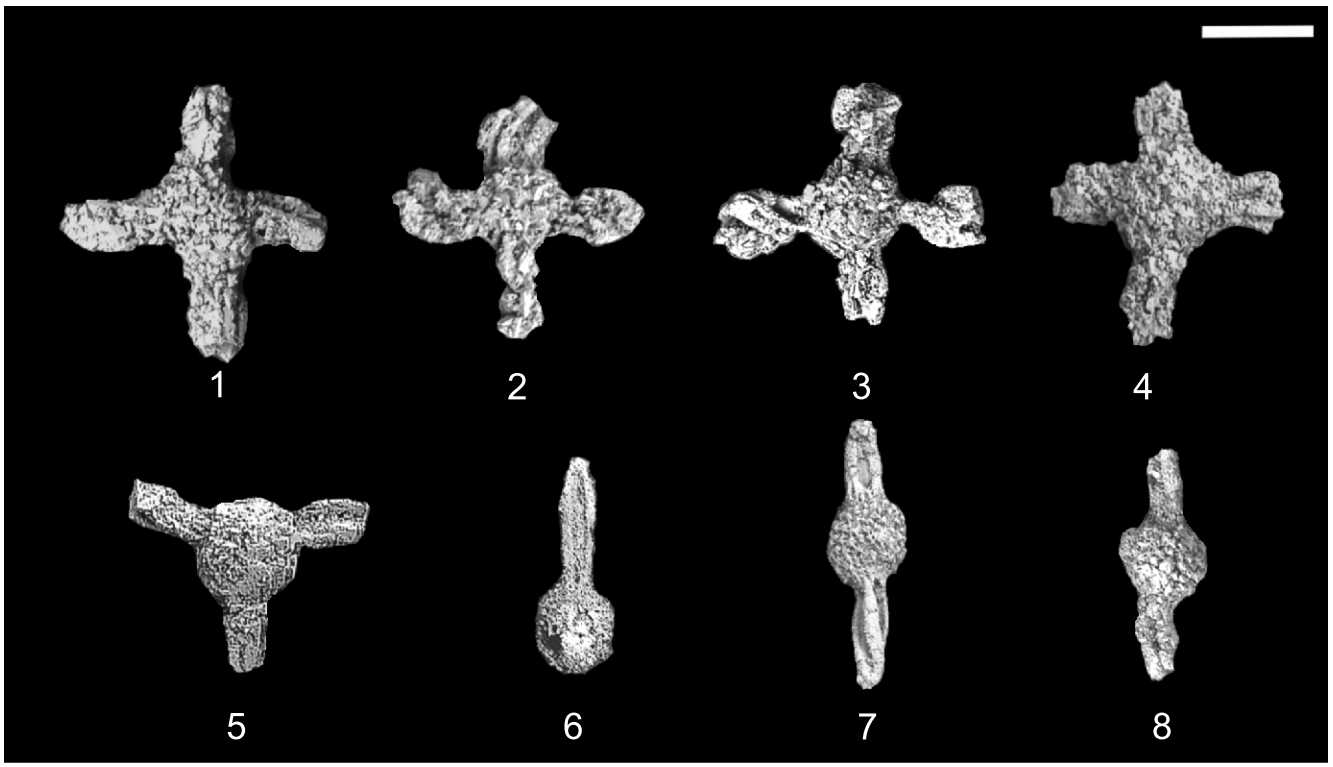

Fig. 15. Radiolaria of late Ladinian age from sample Taş-21 from the Taşönü section

1 – *Muelleritortis cochleata cochleata* (Nakaseko and Nishimura); **2–4 –** *M. expansa* Kozur and Mostler; **5 –***Tritortis kretaensis dispiralis* (Bragin); **6 –** *Pseudostylosphaera* sp. cf. *P. canaliculata* (Bragin); **7, 8 –** *P. imperspicua* (Bragin). Scale bar for specimens: 1 **–** 200, 2–5 – 220, 6 **–** 270, 7, 8 **–** 320μm, respectively

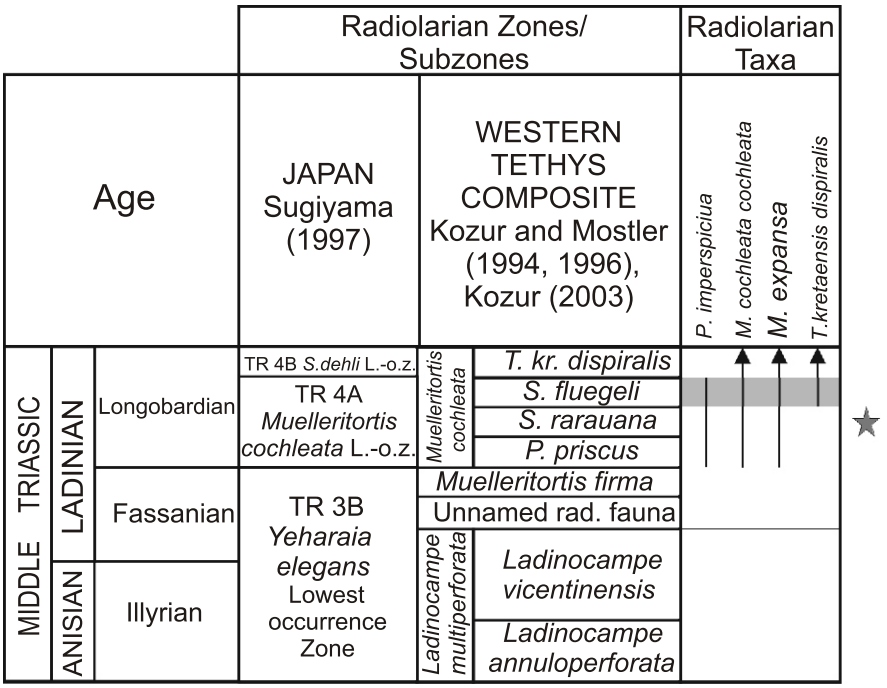

Fig. 16. Stratigraphic distribution of the radiolarian taxa from sample Taş-21 in the Taşönü section

The grey area indicates the range of sample Taş-21 in the upper Ladinian corresponding to the *Spongoserrula fluegeli* Subzone of the *Muelleritortis cochleata* Zone according to Kozur and Mostler (1994, 1996) and Kozur (2003). The Anisian-Ladinian boundary is as defined by Brack et al. (2005). The star symbol at the side of the figure shows the range of sample Zin-2-1 in the Zincancının-2 section studied by Tekin et al. (2025) corresponding to the *Spongoserrula rarauana* Subzone of the *Muelleritortis cochleata* Zone in the middle Upper Ladinian

Table 1

Whole-rock chemical data of the mafic lithologies from the Elmadağ Olistostrome

SAMPLE	ÇAY-1	ÇAY-5	TAŞ-4	TAŞ-5	TAŞ-6	TAŞ-13	ZİN-1-2	ZİN-1-3
Locality	Çayırlık	Çayırlık	Taşönü	Taşönü	Taşönü	Taşönü	Zincancının	Zincancının
SiO_2	46.4	52.5	40.8	39.5	38.6	40.8	31.4	26.5
MgO	1.73	1.97	2.52	1.7	2.37	2.22	4.47	4.67
Al_2O_3	14.75	16	14	13.1	13.35	15	8.89	7.83
Fe_2O_3*	10.45	9.12	11.35	8.74	10.25	10.4	8.7	7.75
CaO	7.92	6.05	10.4	14.7	13.1	9.99	21.9	26.6
Na_2O	5.83	6.24	4.73	4.51	3.76	3.86	1.92	1.37
K_2O	1.98	1.86	0.24	1.06	0.93	2.26	0.02	0.01
Cr_2O_3	0.014	0.005	b.d.	b.d.	b.d.	b.d.	0.048	0.08
TiO_2	1.95	1.62	3.8	3.51	3.61	3.78	1.97	2.07
MnO	0.15	0.14	0.12	0.13	0.15	0.14	0.24	0.15
P_2O_5	0.5	0.55	0.51	0.47	0.46	0.6	0.33	0.48
LOI	7.04	5.66	11.85	14.2	14.25	11.9	19.9	23.3
Total	98.75	101.83	100.37	101.68	100.89	101.02	99.82	100.84
Ni	34	10	5	6	4	12	104	211
Co	18	11	33	29	36	41	32	39
Cr	120	40	10	10	10	10	360	562
Sc	13	12	19	19	18	20	20.7	23.1
V	103	70	270	273	214	257	253	162
Cs	0.55	0.08	0.37	0.69	0.75	3.22	0.06	0.11
Rb	31.5	25.7	4.5	16.9	11.2	41.2	0.6	0.4
Ba	198	471	138	141	168	186.5	26.3	34.9
Sr	167	528	382	352	353	399	268	297
Nb	43.5	62.4	43.2	38.7	39.6	39.6	18.3	17.8
Ta	2.6	3.7	1.8	1.1	0.4	0.5	1.2	1.1
Zr	289	410	290	251	254	260	134	136
Hf	7.1	9.5	7.1	6.5	6.7	6.5	3.72	3.81
Y	36	46.5	29.7	28.9	29.1	29.4	20.9	26.9
La	36.5	51.2	31.8	31.3	28.5	25.5	17.9	21
Ce	75.2	102.5	72.1	68.7	63.5	59.6	39.3	33.5
Pr	10.2	13.2	9.95	9.71	8.96	8.47	5.29	6.01
Nd	40.7	52.2	40.8	40	36.1	35.8	23.6	26.9
Sm	9.14	11.6	9.33	8.87	8.6	8.89	5.5	6.72
Eu	3.06	4.07	2.96	3.06	2.7	2.83	1.72	1.94
Gd	9.44	11.9	8.2	8.84	8.58	8.25	4.86	6.28
Tb	1.29	1.7	1.17	1.21	1.15	1.09	0.72	0.88
Dy	7.67	9.9	6.47	6.71	6.42	6.42	4.24	4.49
Ho	1.47	1.91	1.2	1.26	1.22	1.13	0.76	0.88
Er	3.64	4.99	2.94	3.16	3.06	3	1.8	2.21
Tm	0.49	0.69	0.39	0.41	0.38	0.38	0.22	0.31
Yb	2.95	4.23	2.4	2.51	2.43	2.4	1.48	1.97
Lu	0.46	0.61	0.34	0.36	0.35	0.35	0.21	0.29
Th	4.59	6.06	2.97	2.88	2.8	2.77	1.34	1.26
U	0.65	1.41	1.92	2.15	1.62	1.08	0.51	0.6

* Fe_2O_3 – total iron; b.d. – 'below detection limit

Zincancının section in Tekin et al., 2025) in the Kutludüğün Yayla region (Figs. 6 and 16). According to this study, this radiolarian assemblage indicates the *Spongoserrula rarauana* Subzone of the *Muelleritortis cochleata* Zone according to Kozur and Mostler (1994, 1996) and Kozur (2003), revealing a middle Upper Ladinian (upper Middle Triassic) age (Fig. 16).

GEOCHEMISTRY OF THE MAFIC VOLCANIC ROCKS

ANALYTICAL METHOD

To constrain the petrogenesis and tectonic setting of the Intra-Pontide mafic volcanic rocks exposed in the Elmadağ region (south-east of Ankara), eight samples were analyzed for their whole-rock major and trace element geochemistry at the ALS Laboratories (Dublin; Table 1).

Samples were collected from the same stratigraphic sections used for palaeontological dating, namely the Taşönü, Çayırlık and Zincancının-1 sections. Dissolution of samples for major and most trace elements was accomplished by lithium-tetraborate fusion, while for the others, multi-acid dissolution was employed. The samples were subsequently digested using dilute nitric acid and measured by ICP-AES for major elements and ICP-MS for trace elements. Based on standards and duplicates, the analytical accuracy and precision were better than 5% for most elements. All the oxide concentrations given below were calculated on an anhydrous basis.

RESULTS

Given the low-grade alteration of the samples, we employed the classification diagram of Winchester and Floyd (1977), which relies on immobile element ratios (Fig. 17). Based on this plot, all samples were classified as alkaline basalts, with high

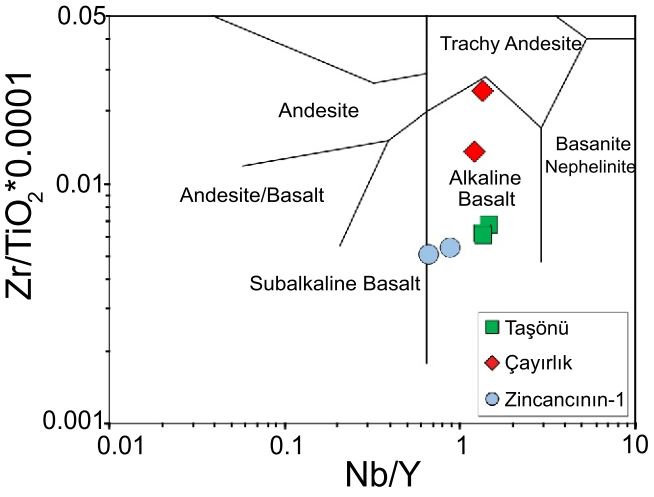

Fig. 17. Immobile element-based chemical classification of the mafic lithologies from the Elmadağ Olistostrome (after Winchester and Floyd, 1977)

Nb/Y ratios. The samples display a broad range of SiO_2 (34.2–54.7 wt.%). The Çayırlık samples have the highest values (50.6–54.7 wt.%), while those from the Zincancının-1 section show the lowest, falling below 40 wt.%. Most of of the Çayırlık samples are either close to or below 4 wt.% MgO, while the Zincancının-1 samples have MgO contents exceeding 5 wt.%. The samples from the Taşönü section show the highest TiO_2 concentrations (average 4.2 wt.%), whereas other localities have lower averages (~2.2 wt.%). While most samples contain ~16 wt.% Al_2O_3, those from the Zincancının-1 section show markedly lower values (10.1–11.1 wt.%).

On the multi-element and rare earth element (REE) plots (Fig. 18), all samples display enrichment in incompatible elements and show similar HREE fractionation. When the entire dataset is considered, absolute abundances vary widely. In detail, the Çayırlık samples span a broad range across the entire elemental spectrum. The Zincancının-1 samples are very similar in terms of incompatible element concentrations; however, the variability increases towards less incompatible elements. In contrast, the Taşönü samples display enrichment levels restricted to a narrow interval. A common feature for all samples is the relative Nb enrichment (Nb/Nb*; calculated as $Nb_{PM}/[Th_{PM} \times La_{PM}]^{0.5}$), which ranges between 1.2 and 1.6. This feature becomes most prominent for the Taşönü samples (Nb/Nb* = 1.4–1.6), which also exhibit positive Ti anomalies (Ti/Ti* = 1.1–1.3, calculated as $Ti_{PM}/[Eu_{PM} \times Gd_{PM}]^{0.5}$). In contrast, the samples from the Çayırlık section display significant negative Ti anomalies (Ti/Ti* = 0.3–0.6).

DISCUSSION

POST-MELTING MODIFICATIONS

The influence of low-grade hydrothermal alteration on the samples is also evident in the geochemistry, as indicated by the loss on ignition (LOI) values reaching up to 19.9 wt.%. During water-rock interaction, some elements can be mobilized, leading to modifications of the pristine chemistry (e.g., Humpris and Thompson, 1978). To test this idea, selected elements were plotted against Zr (Fig. 19), which is known as a highly stable element (i.e., immobile) during low-grade alteration (e.g., Pearce, 1975). In the diagrams, high-field-strength elements (HFSE) (e.g., Nb, Ti, Th, REE) show linear trends, whereas low-ionic potential elements (e.g., Sr, K, and Ba) have a scattered distribution with low correlation. This suggests that while HFSE have largely remained immobile in the samples, the distribution of low-ionic potential elements has been modified through alteration.

SiO_2 displays a broad variation that might initially be attributed to fractional crystallization. However, its strong correlation with LOI (not shown) suggests post-magmatic modification. Notably, the most silica-rich samples show the lowest LOI values. Therefore, while the high-silica end of the spectrum likely represents evolved compositions, the lower values appear to be controlled by alteration. This issue can also be assessed using Co and TiO_2, which are stable during low-grade alteration. Co concentrations range from 11 to 50 ppm, with the lowest values observed in the relatively Si-rich samples. Also, these silica-rich samples have the lowest TiO_2 contents and display prominent negative Ti anomalies on a multi-element diagram (Fig. 18), reinforcing the interpretation that the high-silica end represents more evolved compositions. On the other hand, the lack of Ti anomaly in the other samples may suggest that they are relatively more primitive than those from the Çayırlık section. However, since Co concentrations remain significantly lower than those of primary magmas, even these samples appear to have been modified by fractional crystallization.

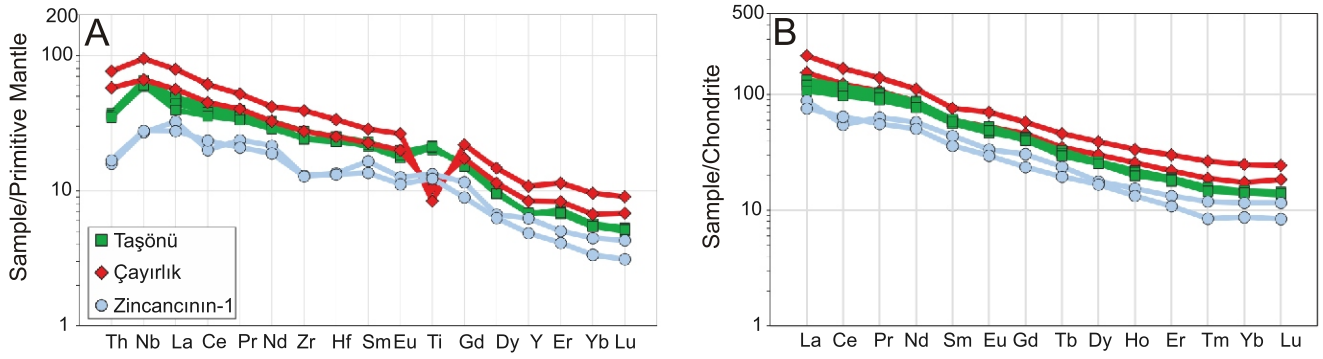

Fig. 18. Multi-element and REE patterns of the mafic lithologies from the Elmadağ Olistostrome

Normalization data for the primitive mantle and chondrite are from McDonough and Sun (1995) and Sun and McDonough (1989), respectively

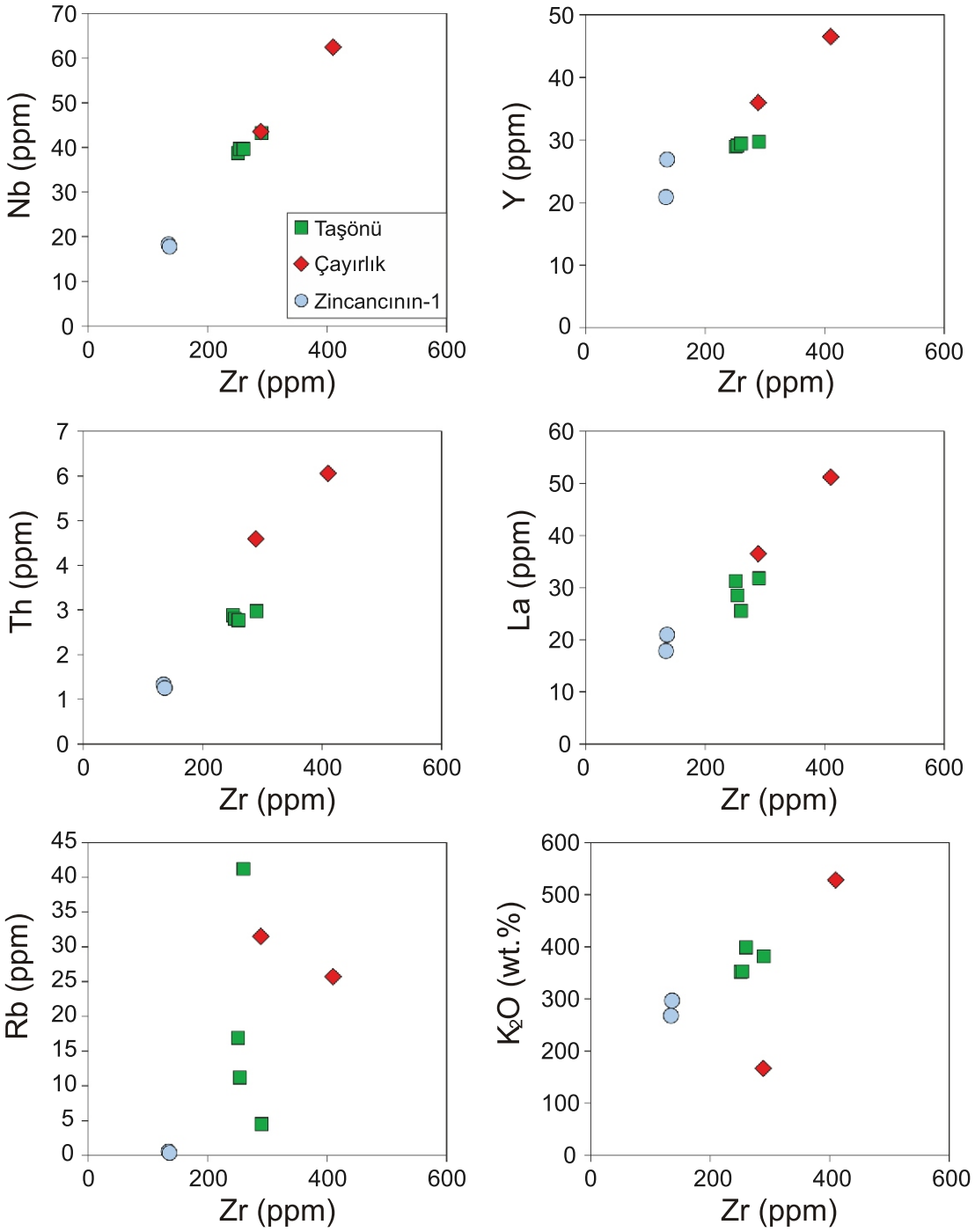

Fig. 19. Plots of selected elements against zirconium for the mafic lithologies from the Elmadağ Olistostrome

NATURE OF THE SOURCE REGION

All samples have high Nb/Nb* values (1.2–1.6), coupled with low Th/Nb and La/Nb ratios (Fig. 20A). Among these elements, Th and La are non-conservative during the subduction processes and are added to the mantle wedge. In contrast, Nb is highly conservative; it is retained in the oceanic crust without being mobilized by slab-derived melts/fluids (Pearce and Peate, 1995). Therefore, melts derived from mantle sources metasomatized by slab-derived materials will be characterized by high Th/Nb and La/Nb ratios. While such ratios are typical of subduction-related melts, such as those from arcs (e.g., Pearce, 1983), this is in strong contrast with the samples studied, which show Nb enrichment (relative to Th and La; Fig. 18A). This suggests that the samples lack a subduction component. Also, since the continental crust shares, in general, geochemical signatures with subduction-derived materials (e.g., high Th/Nb and La/Nb; Taylor and McLennan, 1995), the low Th/Nb, La/Nb, and high Nb/Nb* ratios may preclude continental crustal input in the samples. Therefore, the Nb enrichment in the mantle source of the samples is neither subduction-related nor due to crustal contamination. Rather, it can be attributed to the involvement of recycled mantle materials, such as oceanic crust and oceanic lithospheric mantle (McDonough, 1991; Sayit, 2023).

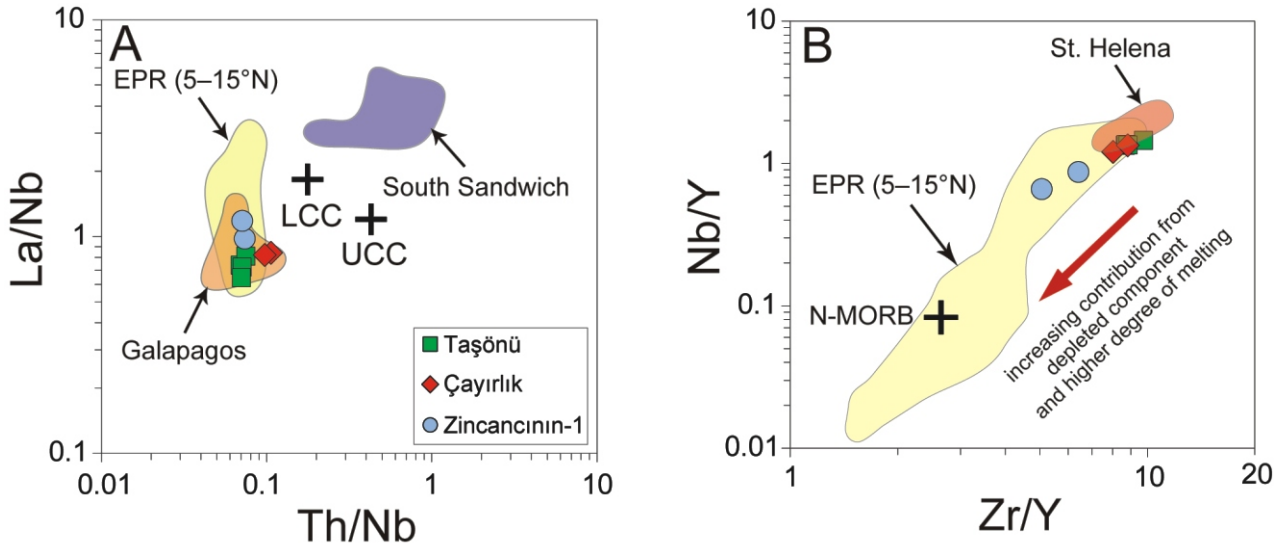

Fig. 20. Plots of A – Th/Nb vs. La/Nb and B – Zr/Y vs Nb/Y for the mafic lithologies from the Elmadağ Olistostrome

Data sources: South Sandwich from Pearce et al. (1995), EPR data from Niu and Batiza (1997); Galapagos from Saal et al. (2007); St. Helena from Kawabata et al. (2011)

All samples show OIB-like trace element patterns (Fig. 18). As a first-order approximation, this may eliminate the strong involvement of a depleted mantle source. To assess this issue in greater detail, we use Zr-Nb-Y systematics, which is based on immobile elements with different incompatibilities during upper mantle melting (Nb-Zr-Y, in order of decreasing incompatibility) (e.g., Sun and McDonough, 1989). Due to the more incompatible nature of Nb, the depleted mantle domains have a deficiency of this element relative to Zr and Y (e.g., Workman and Hart, 2005). Similarly, since Zr is more incompatible than Y, such domains are characterized by Zr depletion relative to Y. Regarding Y, the relative depletion becomes even more significant if garnet remains as a residual phase during melting (e.g., McKenzie and O'Nions, 1991). Thus, depleted mantle domains and their high-degree melt products are characterized by low Nb/Zr, Zr/Y and Nb/Y ratios (e.g., East Pacific Rise, ultra-depleted MORB, sample R74-6; Nb/Zr = 0.01, Zr/Y = 1.5, Nb/Y = 0.01; Niu and Batiza, 1997). This contrasts with undepleted or enriched reservoirs, which have high Zr/Y and Nb/Y ratios (e.g., primitive mantle, Nb/Zr = 0.06, Zr/Y = 2.4, Nb/Y = 0.2; McDonough and Sun, 1995). The samples studied display a range of these ratios, all of which are significantly higher than those of N-MORB (Average values; Nb/Zr = 0.15, Zr/Y = 8.5, Nb/Y = 1.3; Fig. 20B). Such high ratios are comparable with those of ocean island basalts (OIBs; Average OIB; Nb/Zr = 0.17, Zr/Y = 9.7, Nb/Y = 1.7; Sun and McDonough, 1989), which are regarded as including enriched mantle components (relative to the depleted mantle) characterized by recycled crustal/lithospheric materials (e.g., Niu and O'Hara, 2003; Jackson et al., 2007; Salters and Sachi-Kocher, 2010; Sayit, 2023).

A notable feature of the samples from the Taşönü section is their high degree of relative Nb enrichment. This feature, also called the 'Nb-kick' (McDonough, 1991), is associated with low Th/Nb and La/Nb ratios, and is particularly common among melts with FOZO/C- and HIMU-like isotopic signatures from mid-ocean ridges and OIBs (e.g., Jackson et al., 2008; Sayit, 2013). Recently, some Tethyan mafic lithologies of Middle Triassic age from a megablock in the Imrahor region (east of Ankara, Central Anatolia) (now identified as a part of the Elmadağ Olistostrome *sensu* Tekin et al., 2024) were identified to have high Nb positive anomalies (up to 2.1) and are suggested to display FOZO/C-like characteristics (Sayit, 2023). The samples from the Taşönü section have somewhat similar trace element signatures, implying that they may have tapped the FOZO/C-like component to a greater extent compared to the other samples in this study. The positive Ti anomalies of the Taşönü samples, a feature also typical of FOZO-like melts, further support this interpretation.

DISCUSSION

AGE CONSIDERATIONS AND CORRELATIONS

Mafic lithologies (predominantly basalts), which occur as blocks, constitute a relatively minor component of the Elmadağ Olistostrome. Akyürek et al. (1984) mapped these lithologies beneath the Ortaköy Formation, assigning a Middle-Upper Triassic age based on the occurrence of *Meandrospira dinarica* Kochansky-Devidé and Pantić, *Glomospira* sp., *Trochammina* sp., and *Endothyra* sp. taxa. Even though *Meandrospira dinarica* is considered a characteristic Anisian species of the Tethyan realm (e.g., Rettori, 1995; Kobayashi, 1996; Velledits et al., 2011; Altıner et al., 2021), the age of the formation, including limestones intercalated with the mafic volcanic rocks, was given rather broadly as Middle-Upper Triassic. The foraminiferal assemblages recovered and their corresponding ages from the volcanic/carbonate blocks from the Çayırlık, Zincancının-1, and Taşönü sections in this study are consistent with those described by Akyürek et al. (1984; Fig. 21).

Akyürek et al. (1984) interpreted the Ortaköy Formation as stratigraphically transitional to the Elmadağ Formation, considering the latter to comprise siliciclastic deposits and limestone blocks. They assigned a similar age to the Elmadağ Formation based on the presence of *Meandrospira dinarica* Kochansky-Devidé and Pantić, a characteristic Anisian taxon, which was described from carbonate beds within the lower part of the formation. However, the recent study of Tekin et al. (2025) showed that the basaltic and carbonate blocks belong to the Elmadağ Olistostrome (Erol, 1956; Tekin et al., 2024), which overlies the siliciclastic-dominated, non-metamorphic to low-grade metamorphic Dikmen Greywacke (Erol, 1956; Tekin et al., 2024).

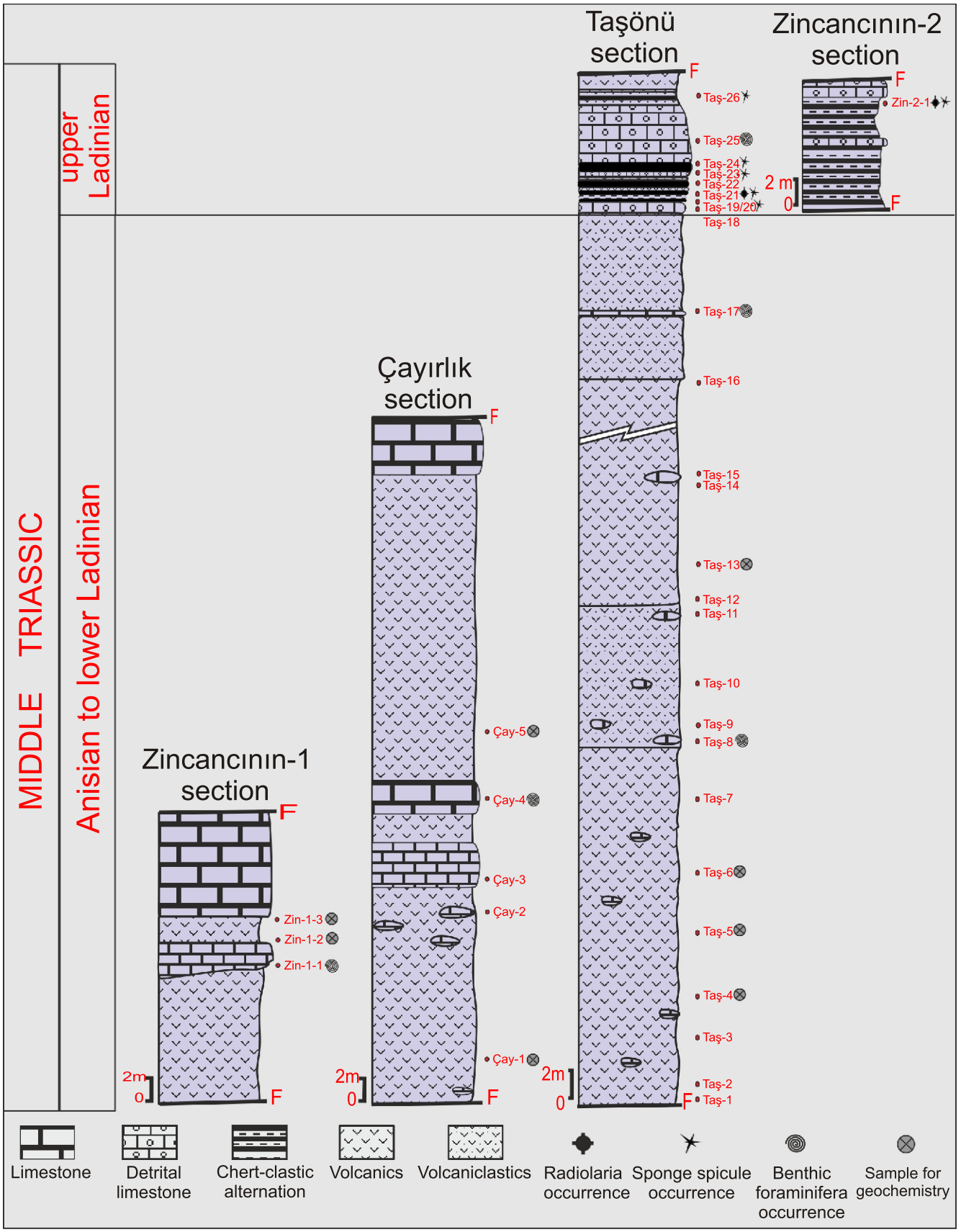

Fig. 21. Correlation of the stratigraphic sections examined in this study (Çayırlık, Zincancının-1 and Taşönü) with the Zincancının-2 section by Tekin et al. (2025)

The volcanic-dominated interval in the lower part of the sequence is of Anisian-lower Ladinian age based on the benthic foraminifera data from the Zincancının-1, Çayırlık and Taşönü sections. The upper part of the sequence is upper Ladinian, based on radiolarian data from spiculite/radiolarian cherts in the Taşönü section (this study) and the Zincancnın-2 section (Tekin et al., 2025)

Tekin et al. (2024) noted that the Dikmen Greywacke lacks carbonate blocks, and that the degree of metamorphism decreases towards its upper levels. Furthermore, our field observations in the Elmadağ region (Ankara, Türkiye) reveal that the upper part of this formation includes rare carbonate interlayers. Therefore, we suggest that the Middle-Upper Triassic carbonate beds within the clastic rocks of the Elmadağ Formation described by Akyürek et al. (1984) may actually belong to the upper levels of the Dikmen Greywacke.

Another Triassic mafic volcanic/carbonate block, located in the Hasanoğlan region (north-east of Ankara), was described by Altıner and Koçyiğit (1993) as an Anisian megablock within the Triassic Karakaya Nappe (equivalent to the Elmadağ Olistostrome of Erol, 1956). According to Altıner and Koçyiğit (1993), this megablock includes pillow lavas, fine-grained pyroclastic rocks and shallow-water carbonates. Palaeontological analyses of these shallow-water carbonates yielded a typical Anisian foraminiferal assemblage, including *Meandrospira dinarica*, *Plammina densa,* and *Glomospirella grandis*. In particular, the occurrence of *Meandrospira dinarica* within the carbonates intercalated with the OIB-type mafic volcanic rocks (Altıner and Koçyiğit, 1993; Sayit and Göncüoğlu, 2009) aligns with the fossil assemblage from the Taşönü section (sample Taş-08) of the Elmadağ Olistostrome described in this study. A similar age was also suggested by Sayit and Göncüoğlu (2009) for the carbonates associated with mafic lithologies in a megablock in the Imrahor region (east of Ankara).

In summary, the similarity between the ages obtained from carbonate layers within OIB-type basaltic blocks in this study and those from previous studies provides important constraints on the age of basalt-bearing sequences in the Elmadağ Olistostrome. These mafic fragments are widespread across central and western Anatolia. For example, the Triassic mafic lithologies in the Biga peninsula (NW Anatolia), formerly called the Nilüfer Unit, are now identified as part of the Elmadağ Olistostrome (Tekin et al., 2024). In this regard, it is critical that these lithologies, previously assumed to be of Palaeotethyan origin, are now interpreted as Neotethyan-derived.

GEODYNAMIC IMPLICATIONS

The geochemical data show OIB-type geochemical signatures with no evidence of slab-derived input, therefore precluding a subduction-related setting. Furthermore, the strong relative Nb enrichment (i.e., low Th/Nb and La/Nb) argues against crustal contamination. Thus, in terms of a pure geochemical standpoint, a non-subduction oceanic setting (e.g., oceanic island/seamount, oceanic plateau, or mid-ocean ridge) is the most plausible explanation. Moreover, the incompatible element-enriched nature of the basalts may eliminate an oceanic plateau origin, which is typically characterized by chondritic or depleted La/Sm ratios (e.g., Fitton and Godard, 2004; Sano et al., 2012).

Some studies (Bingöl et al., 1975; Akyürek et al., 1984; Altıner and Koçyiğit, 1993), based solely on geological observations, suggested a genetic link between the basalts (found as blocks) and the terrigenous deposits (i.e., the Dikmen Greywacke), interpreting the basalts as products of a continental rift. However, the geochemistry of the basalts indicates no crustal contamination, and field observations reveal no primary association between the basalts and the terrigenous deposits, thus precluding a genetic link between them (Sayit and Göncüoğlu, 2009; Sayit et al., 2010; Tekin et al., 2025; this study). Therefore, the combined geochemical and geological evidence strongly favours an oceanic rather than continental origin. The question then arises as to whether these basalts are fragments of an ocean island/seamount or a mid-ocean ridge setting. Incompatible element enrichment and alkaline compositions are typical of ocean islands but rare in mid-ocean ridges. Thus, even though such signatures strongly suggest an ocean island origin, a mid-ocean ridge setting cannot be entirely excluded based on geochemistry alone. However, the intercalation of platform limestones with the basalts provides a compelling argument for an ocean island setting; mid-ocean ridge topography (including off-axis seamounts) does not usually reach the shallow depths required for shallow-water limestone deposition.

All available evidence, therefore, points to an ocean island setting for the origin of the basaltic blocks within the Elmadağ Olistostrome. Similar occurrences, found at several other localities in the Ankara region, as well as to the west (Biga peninsula) (e.g., Akyürek et al., 1984; Okay et al., 1990, 1991), appear to share this same origin, i.e., ocean island (Sayit and Göncüoğlu, 2009, 2013; Sayit et al., 2010). A similar interpretation has also been suggested for the variably metamorphosed mafic lithologies of the Nilüfer Unit *sensu* Okay et al. (1990, 1991) (e.g., Pickett and Robertson, 1996; Sayit et al., 2010). Regarding the Ankara region, at all localities (also including the Imrahor and Hasanoğlan regions reported by Altıner and Koçyiğit, 1993; Sayit and Göncüoğlu, 2009), basalts are intimately associated with platform limestones. Pelagic limestones, on the other hand, are absent. In this context, the platform limestones likely represent reefs that were deposited on the top of an ocean island during its subsidence. This depositional environment is well-observed in the Çayırlık section, where a thick sequence of interfingered basalt-limestone is present. In the Taşönü section, the basaltic lavas include limestone lenses, but this alternation passes into the spiculite/radiolarian cherts and detrital limestones of upper Ladinian age. We think that these detrital limestones are external to the main basalt-limestone association and were supplied from a different source. It is critical that the uppermost pillow basalts are not followed by volcaniclastic facies, which are purely derived from the fragmentation of basalt. Instead, the pillow lava sequence is interrupted by a sedimentary package that begins with a volcanogenic conglomerate with limestone clasts. Within this package, which is mainly carbonate-dominated (with subordinate chert), volcaniclastic rocks are interbedded with either chert or detrital limestone. Also, while some detrital limestones contain basalt clasts, others comprise Carboniferous and Permian clasts. Based on these observations, it seems that this sedimentary package was deposited on top of the basaltic lavas, but contains exotic material supplied to the volcanic system from somewhere else.

Within a broader geodynamic context, the basaltic blocks characterize the fragments of Middle Triassic ocean islands from the Intra-Pontide Ocean (Fig. 22). While the Intra-Pontide Ocean was initially thought to have opened during the Early Jurassic (Şengör and Yılmaz, 1981), the finding of Middle-Upper Triassic radiolarians suggested that the opening of the Intra-Pontide basin is pre-Jurassic (Tekin et al., 2012). A pre-Jurassic opening is also consistent with the Middle-Late Jurassic subduction in the Intra-Pontide realm (Göncüoğlu et al., 2012; Okay et al., 2014; Marroni et al., 2014; Çimen et al., 2016, 2017; Frassi et al., 2018). The Upper Triassic eclogite exposed in Bandırma (Biga peninsula, NW Türkiye), which was previously interpreted in the context of the Karakaya Complex (Okay and Monie, 1997), now appears to be linked to the Intra-Pontide events in the light of new data. The reinterpretation of this eclogite is critical because it implies that the Late Triassic subduction occurred within the Intra-Pontide basin, rather than within Palaeotethys. The Dodurga Pluton, which is interpreted

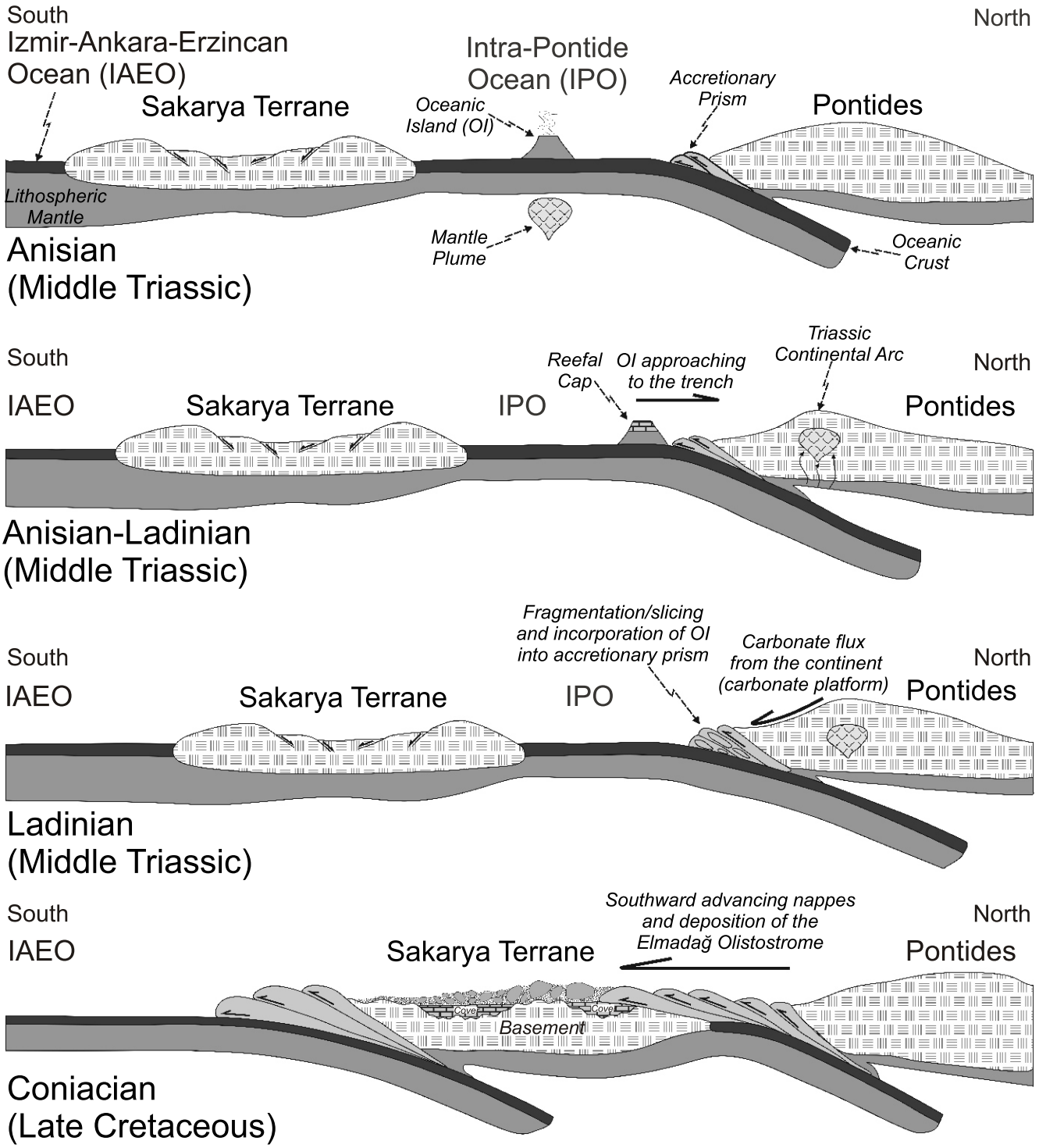

Fig. 22. Cartoon model illustrating the geodynamic evolution of the ocean islands within the Intra-Pontide Ocean during the Anisian to Ladinian timespan, and the subsequent transport and deposition of the Elmadağ Olistostrome carrying these ocean island fragments during the Conician

to represent a Middle Triassic continental arc (239 Ma; Ballato et al., 2018; Çimen, 2020), is also consistent with this view and suggests that the subduction was possibly taking place in the Intra-Pontide Ocean as early as the Middle Triassic. Collectively, these data suggest that the Intra-Pontide was probably a mature oceanic basin already before the Middle Triassic. In a recent study, Tekin et al. (2025) suggested that the rifting of the Intra-Pontide basin may have occurred during the middle-late Permian, based on the presence of palaeontological data obtained from limestone/chert pebbles/blocks at Kutludüğün Yayla, SE Ankara.

When the Middle Triassic ocean islands are integrated into this geodynamic picture, it can be suggested that the Intra-Pontide Ocean was wide enough during the Anisian (Middle Triassic) to develop mature oceanic lithosphere and oceanic islands (Fig. 22). The geochemical features observed are consistent with a plume source, which possibly involved FOZO- and EM-type components. Traces of Triassic OIB-type magmatism are also encountered in the other Tethyan branches (e.g., Lapierre et al., 2007; Varol et al., 2007; Bortolotti et al., 2013). This idea is also consistent with wide-scale plume-related magmatism across the Tethyan realm (e.g., Wilson and Guiraud, 1998; Sayit, 2013). During the Anisian-Ladinian (Fig. 22), the Intra-Pontide oceanic lithosphere was subducting northwards beneath the Pontides, as reflected by the Dodurga continental arc magmatism (Çimen, 2020). With ongoing subduction and subsequent motion of the lithosphere, these ocean islands drifted away from the plume source. Consequently, they subsided to or below sea level, allowing the deposition of shallow-water platform carbonates (syndepositional with basalts) as barrier reefs. During the late Ladinian, exotic sedimentary material, including detrital limestone, was deposited atop the Anisian ocean island sequence. Considering that the detrital limestone includes Devonian to Permian limestone clasts, it is unlikely that such older carbonate material was derived from the ocean island itself. Therefore, the detrital material seems most likely to be continent-derived. We propose that during the late Ladinian, the oceanic islands became fragmented, sliced, and incorporated into the accretionary prism, while the detrital carbonate was supplied from the continental margin.

From the late Ladinian onwards (Fig. 22), the Intra-Pontide Ocean experienced several episodes of subduction, resulting in continental and intra-oceanic arc magmatism (e.g., Okay et al., 2014; Çimen et al., 2016, 2017). During the Late Cretaceous, the Intra-Pontide Ocean was closed (e.g., Tüysüz, 2018; Marroni et al., 2020), which was followed by the southwards nappe emplacement. The Elmadağ Olistostrome was deposited in front of these nappes, within trench-like basins (e.g., Gawlick et al. 1999), and covered an extensive area, stretching from western to Central Anatolia. During the Coniacian, the deposition of the Elmadağ Olistostrome was completed, and its southern extent blanketed the basement (the Dikmen Greywacke) and Jurassic-Cretaceous carbonate-dominated cover of the Sakarya Continent, in addition to the accretionary material of the IAE Ocean (Tekin et al., 2024; Fig. 22).

CONCLUSIONS

The Elmadağ Olistostrome, of the Intra-Pontide realm, contains blocks of basaltic volcanic/volcaniclastic rocks intercalated with platform limestones. The basalts show OIB-type geochemical signatures with no trace of subduction input or crustal contamination. When the geological and geochemical characteristics are taken into account, these basaltic fragments appear to represent ocean islands formed during the Anisian-early Ladinian (Middle Triassic) within the Intra-Pontide Ocean. With ongoing subduction in the Ladinian, these ocean islands were integrated into the accretionary prism at the southern continental margin of the Pontides. Later, following the Late Cretaceous closure of the Intra-Pontide Ocean, the Elmadağ Olistostrome was deposited in front of southward-verging nappes and blanketed the deposits of the Sakarya Continent and the ophiolitic mélange of the IAE Ocean in the Coniacian.

Acknowledgements. The authors gratefully acknowledge the financial support provided by Hacettepe University, Scientific Research Project Department (Project No: FHD-2022-20129). The comments and suggestions from Ioan Bucur and an anonymous reviewer are greatly appreciated.

REFERENCES

Akyürek, B., Bilginer, E., Akbaş, B., Hepşen, N., Pehlivan, Ş., Sunu, O., Soysal, Y., Dağer, Z., Çatal, E., Sözeri, B., Yıldırım, H., Hakyemez, Y., 1984. The basic geological properties of the Ankara-Elmadağ-Kalecik region (in Turkish with English summary). Journal of Geological Engineering, **20**: 31–46.

Altıner, D., Koçyiğit, A., 1993. Third remark on the geology of the Karakaya basin. An Anisian megablock in northern central Anatolia: micropaleontologic, stratigraphic and tectonic implications for the rifting stage of Karakaya basin, Turkey. Revue de Paléobiologie, **12**: 1–17.

Altıner, D., Koçyiğit, A., Farinacci, A., Nicosia, U., Conti, M.A., 1991. Jurassic-Lower Cretaceous stratigraphy and paleogeographic evolution of the southern part of northwestern Anatolia. Geologica Romana, **27**:13–80.

Altıner, D., Payne J.L., Lehrmann, D.J., Özkan-Altıner, S., Kelley, B.M., Summers, M.M., Yu, M., 2021. Triassic foraminifera from the Great Bank of Guizhou, Nanpanjiang Basin, south China: taxonomic account, biostratigraphy, and implications for recovery from end-Permian mass extinction. Journal of Paleontology, **95**: 1–53; https://doi.org/10.1017/jpa.2021.10

Apthorpe, M., 2003. Early to lowermost Middle Triassic foraminifera from the Locker Shale of Hampton-1 well, Western Australia. Journal of Micropalaeontology, **22**: 1–27; https://doi.org/10.1144/jm.22.1.1

Ballato, P., Parra, M., Schildgen, T.F., Dunkl, I., Yıldırım, C., Özsayın, E., Sobel, E.R., Echtler, H., Strecker, M.R., 2018. Multiple exhumation phases in the central Pontides (N Turkey): new temporal constraints on major geodynamic changes associated with the closure of the Neo-Tethys Ocean. Tectonics, **37**: 1831–1857; https://doi.org/10.1029/2017TC004808

Brack, P., Rieber, H., Nicora, A., Mundil, R., 2005. The Global Boundary Stratotype Section and Point (GSSP) of the Ladinian stage (Middle Triassic) at Bagolino (southern Alps, northern Turkey) and its implications to for the Triassic time scale. Episodes, **28**: 233–244; https://doi.org/10.18814/epiiugs/2005/v28i4/001

Beccaletto, L., Bartolini, A.-C., Martini, R., Hochuli, P.A., Kozur, H., 2005. Biostratigraphic data from the Çetmi Melange, northwest Turkey: palaeogeographic and tectonic implications. Palaeogeography, Palaeoclimatolology, Palaeoecology, **221**: 215–244; https://doi.org/10.1016/j.palaeo.2005.02.011

Bedi, Y., Vasilev, E., Dabovski, C., Ergen, A., Okuyucu, C., Doğan, A., Tekin, U.K., Ivanova, D., Boncheva, I., Lakova, I., Sachanski, V., Kuşcu, I., Tuncay, E., Saydam-Demiray, G., Soycan, H., Göncüoğlu, M.C., 2013. New age data from the tectonostratigraphic units of the Istranca ''Massif" in NW Turkey: a correlation with SE Bulgaria. Geologica Carpathica, **64**: 255–277; https://doi.org/10.2478/geoca-2013-0019

Berra, F., Rettori, R., Bassi, D., 2005. Recovery of carbonate platform production in the Lombardy Basin during the Anisian: paleoecological significance and constrain on paleogeographic evolution: Facies, **50**: 615–627; https://doi.org/10.1007/S10347-004-0043-4

Bingöl, E., Akyürek, B., Korkmazer, B., 1975. The geology of the Biga peninsula and some features of the Karakaya Formation (in Turkish with English summary). In: Proceedings of the 50th Anniversary of the Turkish Republic Earth Science Congress: 70–77. Institute of the Mineral Research and Exploration of Turkey Publications.

Bortolotti, V., Chiari, M., Göncüolu, M.C., Marcucci, M., Principi, G., Tekin, U.K., Saccani, E., Tassinari, R., 2013. Age and geochemistry of basalt-chert associations in the ophiolites of the Izmir-Ankara Mélange East of Ankara, Turkey: Preliminary Data. Ofioliti, **38**: 157–173; https://doi.org/10.4454/ofioliti.v38i2.424

Bozorgnia, F., 1973. Paleozoic foraminiferal biostratigraphy of central and East Alborz Mountains, Iran. National Iranian Oil Company, Geological Laboratory Publication, **4**: 1–185.

Bragin, N.Yu., 1991. Radiolaria and Lower Mesozoic units of the USSR, east regions (in Russian with English summary). Trudy Geologicheskogo Instituta (Moskva), **469**.

Bragin, N.Yu., Dronov, A., Raimbekov, Y., 2016. Middle Triassic radiolarians from the Southeastern Pamirs (Republic of Tajikistan). Revue de Micropaléontologie, **59**: 297–310; https://doi.org/10.1016/j.revmic.2016.04.004

Bucur, I.I., Matysik, M., 2020. Dasycladalean green algae and associated foraminifers in Middle Triassic (Lower and Middle Muschelkalk) carbonates of the south-eastern Germanic Basin (Upper Silesia, Poland). Annales Societatis Geologorum Poloniae, **90**: 391–407; https://doi.org/10.14241/asgp.2020.18

Bucur, I.I., Strutinski, C., Pop, D., 1994. Middle Triassic carbonate deposits and calcareous algae from the Sasca Zone (Southern Carpathians, Romania). Facies, **30**: 85–100; https://doi.org/10.1007/BF02536891

Chablais, J., Onoue, T., Martini, R., 2010. Upper Triassic reef-limestone blocks of southwestern Japan: new data from a Panthalassan seamount. Palaeogeography, Palaeoclimatolology, Palaeoecology, **293**: 206–222; https://doi.org/10.1016/j.palaeo.2010.05.022

Cordey, F., De Wever, P., Dumitrica, P., Danelian, T., Kito. N., Vrielynack, B., 1988. Description of some new Middle Triassic radiolarians from the Camp Cove formation, Southern British Columbia, Canada. Revue de Micropaléontologie, **31**: 30–37.

Cózar, P., Vachard, D., Somerville, I.D., Berkhli, M., Medina-Varea, P., Rodríguez, S., Said, I., 2008. Late Viséan-Serpukhovian foraminiferans and calcareous algae from the Adarouch region (central Morocco), North Africa. Geological Journal, **43**: 463–485; https://doi.org/10.1002/gj.1119

Cózar, P., Somerville, I.D., Hounslow, M.W., 2023. Foraminiferal evolution as a basis for the subdivision of the middle Viséan in Europe. Journal of Foraminiferal Research, **53**: 338–361; https://doi.org/10.61551/gsjfr.53.4.338

Çimen, O., 2020. Geochemical characteristics of the adakite-like Dodurga Pluton (Central Pontides, N Turkey): implications for Middle Triassic continental arc magmatism in southern Black Sea region. International Jounal of Earth Sciences, **109**: 809–829; https://doi.org/10.1007/s00531-020-01831-x

Çimen, O., Göncüoğlu, M.C., Sayit, K., 2016. Geochemistry of the metavolcanic rocks from the Çangaldağ Complex in the central Pontides: implications for the Middle Jurassic arc-back-arc system in the Neotethyan Intra-Pontide Ocean. Turkish Journal of Earth Sciences, **25**: 491–512; https://doi.org/10.3906/yer-1603-11

Çimen, O., Göncüoğlu, M.C., Simonetti, C., Sayit, K., 2017. Whole rock geochemistry, Zircon U-Pb and Hf isotope systematics of the Çangaldağ Pluton: evidences for Middle Jurassic Continental Arc Magmatism in the Central Pontides, Turkey. Lithos, **290**: 136–155; https://doi.org/10.1016/j.lithos.2017.06.020

De Wever, P., Dumitrica, P., Caulet, J.P., Nigrini, C., Caridroit, M., 2001. Radiolarians in the sedimentary record. Gordon and Breach Science Pub., London; https://doi.org/10.1201/9781482283181

Dosztaly, L. 1989. Triassic radiolarians from Dallapustza (Mount Darno, N. Hungary). Magyar Állami Földtani Intézet évi jelentése 1988: 193–201.

Emmerich, A., Zamparelli, V., Bechstädt, T., Zühlke, R., 2005. The reefal margin and slope of a Middle Triassic carbonate platform: the Latemar (Dolomites, Italy). Facies, **50**: 573–614; https://doi.org/10.1007/s10347-004-0033-6

Erol, O., 1956. A study of the geology and geomorphology of the region SE of Ankara in Elma Dađý and its surroundings (in Turkish with English summary). Institute of Mineral and Research Explorition of Turkey, Special Publication, Serie D, **9**: 1–99.

Fitton, J.G., Godard, M., 2004. Origin and evolution of magmas on the Ontong Java Plateau. Geological Society Special Publications, **229**: 151–178; https://doi.org/10.1144/GSL.SP.2004.229.01.1

Frassi, C., Marroni, M., Pandolfi, L., Göncüoğlu, M.C., Ellero, A., Otrria, G., Sayit, K., McDonald, C.S., Balestrieri, M.L., Malasoma, A., 2018. Burial and exhumation history of the Daday Unit (central Pontides, Turkey): implications for the closure of the Intra-Pontide oceanic basin. Geological Magazine, **155**: 356–376; https://doi.org/10.1017/S0016756817000176

Fugagnoli, A., Posenato, R., 2004. Middle Triassic (Anisian) benthic foraminifera from the Monte Pra' della Vacca/Kühwiesenkopf section, Dont Formation, Braies Dolomites, northern Italy. Bollettino della Societa Paleontologica Italiana, **43**: 347–360.

Flügel, E., 2004. Microfacies of Carbonate Rocks. Analysis, Interpretation and Application. Springer. ISBN: 3 540 22016 X

Gaillot, J., Vachard, D., 2007. The Khuff Formation (Middle East) and time-equivalents in Turkey and south China: biostratigraphy from Capitanian to Changhsingian times (Permian), new foraminiferal taxa, and palaeogeographical implications. Coloquios de Paleontología, **57**: 37–223.

Gale, L., Rettori, R., Martini, R., Smuc, A., Kolar-Jurkovsek, T., Rozic, B., 2011. Duostominidae (Foraminifera, Robertinida) from the Upper Triassic beds of the Slovenian Basin (Southern Alps, Slovenia). Rivista Italiana di Paleontologia e Stratigrafia, **117**: 375–397; https://doi.org/10.13130/2039-4942/5982

Gale, L., Kolar-Jurkovšek, T., Šmuc, A., Rožič, B., 2012. Integrated Rhaetian foraminiferal and conodont biostratigraphy from the Slovenian Basin, eastern southern Alps. Swiss Journal of Geosciences, **105**: 405–462; https://doi.org/10.1007/s00015-012-0117-1

Gale, L., Kadivec, K., Vrabec, M., Celarc, B., 2023. Sediment infill of the Middle Triassic half-graben below Mt. Vernar in the Julian Alps, Slovenia. Geologia Croatica, **76**: 1–12; https://doi.org/10.4154/gc.2023.03

Gawlick, H.J., Frisch, W., Vecsei, T., Steiger, T., Böhm, F., 1999. The change from rifting to thrusting in the Northern Calcareous Alps as recorded in Jurassic sediments. Geologische Rundschau, **87**: 644–657; https://doi.org/10.1007/s005310050237

Gorican, S., Halamic, J., Grgasovic, T., Kolar-Jurkovsek, T., 2005. Stratigraphic evolution of Triassic arc-backarc system in northwestern Croatia. Bulletin de la Société Géologique de France, **176**: 3–22; https://doi.org/10.2113/176.1.3

Göncüoğlu, M.C., Dirik, K., Kozlu, H., 1997. Pre-Alpine and alpine terranes in Turkey: explanatory notes to the terrane map of Turkey. Annales Geologique de Pays Hellenique, **37**: 515–536.

Göncüoğlu, M.C., Turhan, N., Ţentürk, K., Özcan, A., Uysal, S., Yalınız, M.K., 2000. A geotraverse across NW Turkey: tectonic units of the Central Sakarya region and their tectonic evolution. Geological Society Special Publications, **173**: 139–161; https://doi.org/10.1144/gsl.sp.2000.173.01.06

Göncüoğlu, M.C., Marroni, M., Sayit, K., Tekin, U.K., Ottria, G., Pandolfi, L., Ellero, A., 2012. The Aylı Dağ ophiolite sequence (central-northern Turkey): a fragment of Middle Jurassic oceanic lithosphere within the Intra-Pontide Suture Zone. Ofioliti, **37**: 77–92; https://doi.org/10.4454/ofioliti.v37i2.407

Groves, J.R., Boardman, H., 1999. Calcareous smaller foraminifers from the lower Permian Council Grove Group near Hooser, Kansas. Journal of Foraminiferal Research, **29**: 243–262.

Groves, J.R., Yue, W., Yuping, Q., Richards, B.C., Ueno, K., Xiangdong, W., 2012. Foraminiferal biostratigraphy of the Visean–Serpukhovian (Mississippian) boundary interval at slope and platform sections in southern Guizhou (South China). Journal of Paleontology, **86**: 753–774; https://doi.org/10.2307/23254503

Ha, T.T.N., Takayanagi, H., Ueno, K., Asahara, Y., Yamamoto, K., Iryu, Y., 2019. Litho-, bio-, and chemostratigraphy of the Middle Triassic carbonate succession in the north-central coast region of Vietnam. Progress in Earth and Planetary Science, **6**, 47; https://doi.org/10.1186/s40645-019-0293-y

Hamdi, B., Sadeghi, A., Kohansa, E, Ardestani, M.S., Balmaki, B., 2009. Biostratigraphy of the Ruteh Formation at Harijan section (central Alborz) northern Iran using foraminifera and conodont. Nature Precedings, **459**: 1–8; https://doi.org/10.1038/npre.2009.3376.1

Hauser, M., Martini, R., Burns, S., Dumitrica, P., Krystyn, L., Matter, A., Peters, T., Zaninetti, L., 2001. Triassic stratigraphic evolution of the Arabian-Greater India embayment of the southern Tethys Margin. Eclogae Geologicae Helvetiae, **94**: 29–62.

He, Y., 1984. Middle Triassic Foraminifera from central and southern Guizhou, China (in Chinese with English summary). Acta Palaeontologica Sinica, **23**: 420–431.

He, Y., Wang, L., 1990. Triassic foraminifera from Yushu Region, Qinghai, in Devonian–Triassic stratigraphy and palaeontology from Yushu Region of Qinghai, China, Part 1 (in Chinese with English summary): 59–96. Nanjing University Press, Nanjing.

Hips, K., 2022. Sedimentary aspects of the onset of Middle Triassic continental rifting in the western end of Neotethys; inferences from the Silica and Torna Nappes, NE Hungary: a review. Facies, **68**, 8; https://doi.org/10.1007/s10347-022-00646-3

Humphris, S.E., Thompson, G., 1978. Trace element mobility during hydrothermal alteration of oceanic basalts. Geochimica et Cosmochimica Acta, **42:** 127–136 https://doi.org/10.1016/0016-7037(78)90222-3

Jackson, M.G., Hart, S.R., Koppers, A.A., Staudigel, H., Konter, J., Blusztajn, J., Kurz, M., Russell, J.A., 2007. The return of subducted continental crust in Samoan lavas. Nature, **448**: 684–687; https://doi.org/10.1038/nature06048

Jackson, M.G., Hart, S.R., Saal, A., Schimizu, N., Kurz, M.D., Blusztajn, J.S., Skovgaard, A.C., 2008. Globally elevated titanium, tantalum, and niobium (TITAN) in ocean island basalts with high $^{3}He/^{4}He$. Geochemistry, Geophysics, Geosystems, **9**, Q04027; https://doi.org/10.1029/2007GC001876

Kametaka, M., Kojima, S., Kemkin, I.V., 1997. Mesozoic radiolarians from the Taukha terrane, Far East Russia. News of Osaka Micropaleontologists, Special Volume, **10**: 143–154.

Kawabata, H., Hanyu, T., Chang, Q., Kimura, J.-I., Nichols, A.R.L., Tatsumi, Y., 2011. The petrology and geochemistry of St. Helena alkali basalts: evaluation of the oceanic crust-recycling model for HIMU OIB. Journal of Petrology, **52**: 791–838; https://doi.org/10.1093/petrology/egr003

Kobayashi, F., 1996. Middle Triassic (Anisian) foraminifers from the Kaizawa Formation, southern Kanto Mountains, Japan. Transactions and Proceedings of the Palaeontological Society of the Japan, New Series, **183**: 528–539; https://doi.org/10.14825/prpsj1951.1996.183_528

Kobayashi, F., 2008. Early Anisian (Triassic) foraminifers from the Hiraki Formation of the Maizuru Terrane in the Tatsuno-Aioi area, Hyogo Prefecture, Japan. The Journal of Geological Society of Japan, **114**: 80–87; https://doi.org/10.5575/geosoc.114.80

Kobayashi, F., Vachard D., 2022. Carboniferous foraminifers and biostratigraphy of lower Akiyoshi Limestone (Japan). Revue de Paléobiologie, **41**: 99–239; https://doi.org/10.5281/zenodo.6858353

Kobayashi, F., Martini, R., Zaninetti, L., 2005. Anisian foraminifers from allochthonous limestones of the Tanoura formation (Kurosegawa Terrane, West Kyushu, Japan). Geobios, **38**: 751–763; https://doi.org/10.1016/j.geobios.2004.06.004

Kobayashi, F., Martini, R., Rettori, R., Zaninetti, L., Ratanasthien, B., Saegusa, H., Nakaya, H., 2006. Triassic foraminifers of the Lampang Group (northern Thailand). Journal of Asian Earth Sciences, **27**: 312–325; https://doi.org/10.1016/j.jseaes.2005.04.003

Koehn-Zaninetti, L., 1969. Les foraminifères du Trias de la région de l'Almtal (Haute-Autriche). Jachrbuch der Geologischen Bundesanstalt A Special Volume, **14**: 1–155.

Kozur, H., 1988. Muelleritortiidae n. fam., eine characteristiche longobardische (oberladinische) Radiolarienfamilie, Teil 1. Freiberger Forschungshefte, **419**: 51–61.

Kozur, H., 2003. Integrated ammonoid, conodont and radiolarian zonation of the Triassic and some remarks to stage/substage subdivision and the numeric age of the Triassic stages. Albertiana, **28**: 57–74.

Kozur, H., Mostler, H., 1994. Anisian to middle Carnian radiolarian zonation and description of some stratigraphically important radiolarians. Geologisch-Paläontologische Mitteilungen Innsbruck, **3**: 39–255.

Kozur, H., Mostler, H., 1996. Longobardian (late Ladinian) Muelleritortidae (Radiolaria) from the Republic of Bosnia-Hercegovina. Geologisch-Paläontologische Mitteilungen Innsbruck, **4**: 83–103.

Kukoč, D., Smirčić, D., Grgasović, T., Horvat, M., Belak, M., Japundžić, D., Kolar-Jurkovšek, T., Šegvić, B., Badurina, L., Vukovski, M., Slovenec, D., 2023. Biostratigraphy and facies description of Middle Triassic rift-related volcano-sedimentary successions at the junction of the southern Alps and the Dinarides (NW Croatia). International Journal of Earth Sciences, **112**: 175–1201; https://doi.org/10.1007/s00531-023-02301-w

Lapierre, H., Bosch, D., Narros, A., Mascle, G.H., Tardy, M., Demant, A., 2007. The Mamonia Complex (SW Cyprus) revisited: remnant of Late Triassic intra-oceanic volcanism along the Tethyan southwestern passive margin. Geological Magazine, **144**: 1–19; https://doi.org/10.1017/S0016756806002937

Lehrmann, D.J., Stepchinski, L., Altýner, D., Orchard, M.J., Montgomery, P., Enos, P., Ellwood, B.B., Bowring, S.A., Ramezani, J., Wang, H., Wei, J., Yu, M., Griffiths, J.D., Minzoni, M., Schall, E.K., Li, X., Meyer, K.M., Payne, J.L., 2015. An integrated biostratigraphy (conodonts and foraminifers) and chronostratigraphy (paleomagnetic reversals, magnetic susceptibility, elemental chemistry, carbon isotopes and geochronology) for the Permian–Upper Triassic strata of Guandao section, Nanpanjiang Basin, South China. Journal of Asian Earth Sciences, **108**: 117–135; https://doi.org/10.1016/j.jseaes.2015.04.030

Leven, E.Ja., Okay, A.I., 1996. Foraminifera from the exotic Permo-Carboniferous limestone blocks in the Karakaya Complex, northwest Turkey. Rivista Italiana di Paleontologia e Stratigrafia, **102**: 139–174.

Mamet, B., 1991. Carboniferous calcareous algae. In: Calcareous Algae and Stromatolites (ed. R. Riding): 370–451. Springer, Berlin.

Mamet, B., 1996. Algues calcaires marines du Paléozoïque Supérieur (Equateur, Bolivie). Annales de la Société Géologique de Belgique, **17**: 155–167.

Marroni, M., Frassi, C., Göncüoğlu, M.C., Di Vincenzo, G., Pandolfi, L., Rebay, G., Ellero, A., Ottria, G., 2014. Late Jurassic amphibolite-facies metamorphism in the Intra-Pontide Suture Zone (Turkey): an eastward extension of the Vardar Ocean from the Balkans into Anatolia? Journal of Geological Society, **171**: 605–608; https://doi.org/10.1144/jgs2013-104

Marroni, M., Göncüoğlu, M.C., Frassi, C., Sayit, K., Pandolfi, L., Ellero, A., Ottria, G., 2020. The Intra-Pontide ophiolites in Northern Turkey revisited: from birth to death of a Neotethyan oceanic domain. Geoscience Frontiers, **11**: 129–149; https://doi.org/10.1016/j.gsf.2019.05.010

Martini, R., Zaninetti, L., Cornée, J.-J., Villeneuve, M., Tran, N., Ta, T.T., 1998. Découverte de foraminifères du Trias dans les calcaires de la région de Ninh Binh (Nord-Vietnam). Comptes Rendus de l'Académie des Sciences Paris, **326**: 113–119; https://doi.org/10.1016/S1251-8050(97)87455-1

McDonough, W.F., 1991. Partial melting of subducted oceanic crust and isolation of its residual eclogitic lithology. Philosophical Transactions of the Royal Society, A **335**: 407–418; https://doi.org/10.1098/rsta.1991.0055

McDonough, W.F., Sun, S.-S. 1995. The composition of the Earth. Chemical Geology, **120**: 223–253; https://doi.org/10.1016/0009-2541(94)00140-4

McKenzie, D., O'Nions, R.K., 1991. Partial melt distributions from inversion of rare earth element concentrations. Journal of Petrology, **32**: 1021–1091; https://doi.org/10.1093/petrology/32.5.1021

Mietto, P., Fratoni, R.P., Perri, M.C., 1991. Spathian and Aegean conodonts from the Capelluzzo Calcarenites of the Monte Facito Group (Lagonegro Sequence, southern Apennines). Memorie di Scienze Geologiche, Universita di Padova, **43**: 305–317.

Miyahigashi, A., Ueno, K., Charoentitirat, T., Kamata, Y., 2012. Foraminiferal assemblage and depositional environment of the Doi Long Formation (Triassic Lampang Group), northern Thailand. Acta Geoscientica Sinica, **33**: 45–49; https://doi.org/10.14863/geosocabst.2012.0_477

Nakaseko, K., Nishimura, A., 1979. Upper Triassic Radiolaria from southwest Japan. Scientific Report, College of General Education, Osaka University, **28**: 61–109.

Nejad, M.E., Vachard, D., Siabeghodsy, A.A., Abbasi, S., 2015. Middle-Late Permian (Murgabian-Djulfian) foraminifers of the northern Maku area (western Azerbaijan, Iran). Palaeontologia Electronica, **18.1.19A**: 1–63; https://doi.org/10.26879/453

Niu, Y., Batiza, R., 1997. Trace element evidence from seamounts for recycled oceanic crust in the Eastern Pacific mantle. Earth and Planetary Science Letters, **148**: 471–483; https://doi.org/10.1016/S0012-821X(97)00048-4

Niu, Y., O'Hara, M.J., 2003. Origin of ocean island basalts: A new perspective from petrology, geochemistry, and mineral physics considerations. Journal of Geophysical Research, **108** (B4), 2209; https://doi.org/10.1029/2002JB002048

Okay, A.I., 1989. Tectonic units in the Pontides, northern Turkey. In: Tectonic Evolution of the Tethyan Region (ed. A.M.C. Şengör): 109–116. Kluwer Academic Publishers; https://doi.org/10.1007/978-94-009-2253-2_6

Okay, A.I., 2000. Was the Late Triassic orogeny in Turkey caused by the collision of an oceanic plateau? Geological Society Special Publications, **173**: 139–161; https://doi.org/10.1144/GSL.SP.2000.173.01.02

Okay, A.I, Altıner, D., 2004. Uppermost Triassic Limestone in the Karakaya Complex-Stratigraphic and Tectonic Significance. Turkish Journal of Earth Sciences, **13**: 187–199.

Okay, A.I., Göncüoğlu, M.C., 2004. The Karakaya Complex: A review of data and concepts. Turkish Journal of Earth Sciences, **13**: 77–95.

Okay, A.I., Monie, P., 1997. Early Mesozoic subduction in the Eastern Mediterranean: Evidence from Triassic eclogite in northwest Turkey. Geology, **25**: 595–598; https://doi.org/10.1130/0091-7613

Okay, A.I., Tüysüz, O., 1999. Tethyan sutures of northern Turkey. Geological Society Special Publication, **156**: 475–515; https://doi.org/10.1144/GSL.SP.1999.156.01.22

Okay, A.I., Siyako, M., Bürkan, B.A., 1990. Geology and tectonic evolution of the Biga peninsula (in Turkish with English summary). Turkish Association of Petroleum Geologists Bulletin, **2**: 83–121.

Okay, A.I., Siyako, M., Bürkan, K.A., 1991. Geology and tectonic evolution of the Biga peninsula, northwest Turkey. Bulletin of the Technical University of Istanbul, **44**:191–256.

Okay, A.I., Sunal, G., Tüysüz, O., Sherlock, S., Keskin, M., Kylander-Clark, A.R.C., 2014. Low-pressure–high-temperature metamorphism during extension in a Jurassic magmatic arc, central Pontides, Turkey. Journal of Metamorphic Geology, **32**: 49–69; https://doi.org/10.1111/jmg.12058

Pearce, J.A., 1975. Basalt geochemistry used to investigate past tectonic environments on Cyprus. Tectonophysics, **25:** 41–67; https://doi.org/10.1016/0040-1951(75)90010-4

Pearce, J.A., 1983. The role of sub-continental lithosphere in magma genesis at active continental margins. In: Continental Basalts and Mantle Xenoliths (eds. C.J. Hawkesworth and M.J. Norry): 230–249. Shiva, Nantwich.

Pearce, J.A., Peate, D.W., 1995. Tectonic implications of the composition of volcanic arc magmas. Annual Review of Earth and Planetary Sciences, **23:** 251–285; https://doi.org/0.1146/annurev.ea.23.050195.001343

Pearce, J.A., Baker, P.E., Harvey, P.K., Luff, I.W., 1995. Geochemical evidence for subduction fluxes, mantle melting and fractional crystallization beneath the South Sandwich Island Arc. Journal of Petrology, **36**: 1073–1109; https://doi.org/10.1093/petrology/36.4.1073

Petrova, L.G., 1981. Foraminifera from the Middle Devonian of the eastern slope of the Urals. Proceedings of the Institute of Geology and Geophysics, Novosibirsk, Nauka, **482**: 81–101

Peyrotty, G., Ueda, H., Peybernes, C., Rettori, R., Martini, R., 2020. Upper Triassic shallow-water carbonates from the Naizawa Accretionary Complex, Hokkaido (Japan): new insights from Panthalassa. Palaeogeography, Palaeoclimatolology, Palaeoecology, **554**, 109832; https://doi.org/10.1016/j.palaeo.2020.109832

Pickett, E.A., Robertson, A.H.F., 1996. Formation of the Late Palaeozoic–Early Mesozoic Karakaya Complex and related ophiolites in NW Turkey by Palaeotethyan subduction-accretion. Journal of the Geological Society, **153**: 995–1009; https://doi.org/10.1144/gsjgs.153.6.099

Pille, L., 2008. Foraminifères et algues calcaires du Mississippien supérieur (Viséen supérieur-Serpoukhovien): rôles biostratigraphique, paléoécologique et paléogéographique aux échelles locale, régionale et mondiale. Thèse de 3e cycle, Université de Lille, 3 volumes.

Rettori, R., 1995. Foraminiferi del Trias inferiore e medio della Tetide: Revisione tassonomica, stratigrafia et interpretazione filogenetica. Université de Genève, Publication of Department of Geology and Paleontology, **18**: 1–147.

Rettori, R., Angiolini, L., Muttoni, G., 1994. Lower and Middle Triassic Foraminifera from the Eros Limestone, Hydra Island, Greece. Journal of Micropaleontology, **13**: 25–46; https://doi.org/10.1144/jm.13.1.25

Rojay, B., 2013. Tectonic evolution of the Cretaceous Ankara Ophiolitic Mélange during the Late Cretaceous to pre-Miocene interval in central Anatolia, Turkey. Journal of Geodynamics, **65**: 66–81; https://doi.org/10.1016/j.jog.2012.06.006

Saal, A.E., Kurz, M.D., Hart, S.R., Blusztajn, J.S., Blichert-Toft, J., Geist, D.J., 2007. The role of lithospheric gabbros on the composition of Galapagos lavas. Earth and Planetary Science Letters, **257**: 391–406; https://doi.org/10.1016/j.epsl.2007.02.040

Salaj, J., Borza, K., Samuel, O., 1983. Triassic foraminifers of the West Carpathians. Geologický Ustav Dionýza Stúra, Bratislava.

Salters, J.M., Sachi-Kocher, A., 2010. An ancient metasomatic source for the Walvis Ridge basalts. Chemical Geology, **273**: 151–167; https://doi.org/10.1016/j.chemgeo.2010.02.010

Sano, T., Shimizu, K., Ishikawa, A., Senda, R., Chang, Q., Kimura, J-I., Widdowson, M., Sager, W.W., 2012. Variety and origin of magmas on Shatsky Rise, northwest Pacific Ocean. Geochemistry, Geophysics, Geosystems, **13**: 1–25; https://doi.org/10.1029/ 2012GC004235

Sayit, K., 2013. Immobile trace element systematics of ocean island basalts: the role of oceanic lithosphere in creating the geochemical diversity. Ofioliti, **38**: 101–120; https://doi.org/10.4454/ofioliti.v38i1.419

Sayit, K., 2023. Insights into the Tethyan mantle heterogeneity: Trace element evidence from the Karakaya Complex, central Anatolia. Geosystems and Geoenvironment, **2**, 100139; https://doi.org/10.1016/j.geogeo.2022.100139

Sayit, K., Göncüoğlu, M.C., 2009. Geochemistry of mafic rocks of the Karakaya Complex, Turkey: evidence for plume involvement in the Palaeotethyan extensional regime during the Middle and Late Triassic. International Journal of Earth Sciences, **98**: 367–385; https://doi.org/10.1007/s00531-007-0251-6

Sayit, K., Göncüoğlu, M.C., 2013. Geodynamic evolution of the Karakaya Mélange Complex, Turkey: a review of geological and petrological constraints. Journal of Geodynamics, **65**: 56–65; https://doi.org/10.1016/j.jog.2012.04.009

Sayit, K., Göncüoğlu, M.C., Furman, T., 2010. Petrological reconstruction of Triassic seamounts/oceanic islands within the Palaeotethys: Geochemical implications from the Karakaya subduction/accretion complex, northern Turkey. Lithos, **119**: 501–511; https://doi.org/10.1016/j.lithos.2010.08.004

Sayit, K., Bedi, Y., Tekin, U.K., Göncüoğlu, M.C., Okuyucu, C., 2017. Middle Triassic back-arc basalts from the blocks in the Mersin Mélange, southern Turkey: implications for the geodynamic evolution of the Northern Neotethys. Lithos, **268–271**: 102–113; https://doi.org/10.1016/j.lithos.2016.10.032

Song, H., Tong, J., Chen, Z.Q., 2011. Evolutionary dynamics of the Permian–Triassic foraminifer size: evidence for Lilliput effect in the end-Permian mass extinction and its aftermath. Palaeogeography, Palaeoclimatolology, Palaeoecology, **308**: 98–110; https://doi.org/10.1016/j.palaeo.2010.10.036

Song, H., Wang, L., Tong, J., Chen, J., Tian, L., Song, H., Chu, D., 2015. Recovery dynamics of foraminifers and algae following the Permian-Triassic extinction in Qingyan, south China. Geobios, **48**: 71–83; https://doi.org/10.1016/j.geobios.2014.11.004

Spandel, E., 1901. Die Foraminiferen des Permo-Carbon von Hooser, Kansas, Nord Amerika. In: Saecular-Feier der Naturhistorischen Gesellschaft in Nürnberg 1801–1901 (eds. S.V. Forster, M. Versen and A. Frankenburger): 175–194. Festschrift. U.E. Sebald, Nürnberg.

Stampfli, G.M., Borel, G.D., 2002. A plate tectonic model for the Paleozoic and Mesozoic constrained by dynamic plate boundaries and restored synthetic oceanic isochrons. Earth and Planetary Science Letters, **196**: 1733; https://doi.org/10.1016/S0012-821X(01)00588-X

Sugiyama, K., 1997. Triassic and Lower Jurassic radiolarian biostratigraphy in the siliceous claystone and bedded chert units of the southeastern Mino Terrane, central Japan. Bulletin of the Mizunami Fossil Museum, **24**: 79–193.

Sun, S.-S., McDonough, W.F., 1989. Chemical and isotopic systematics of oceanic basalts: implications for mantle composition and processes. Geological Society Special Publications, **42**: 313–345; https://doi.org/10.1144/GSL.SP.1989.042.01.19

Şahin, N., Altıner, D., Ercengiz, M.B., 2012. Discovery of Middle Permian volcanism in the Antalya nappes, southern Turkey: tectonic significance and global meaning. Geodinamica Acta, **25**: 286–304; https://doi.org/10.1080/09853111.2013.858949

Şengör, A.M.C., 1979. Mid-Mesozoic closure of Permo-Triassic Tethys and its implications. Nature, **279**: 590593; https://doi.org/10.1038/279590a0

Şengör, A.M.C., Yılmaz, Y., 1981. Tethyan evolution of Turkey: a plate tectonic approach. Tectonophysics, **75**: 181–241; https://doi.org/10.1016/0040-1951(81)90275-4

Şengör, A.M.C., Yilmaz, Y., Sungurlu, O., 1984. Tectonics of the Mediterranean Cimmerides: nature and evolution of the western termination of Paleo-Tethys. Geological Society, London, Special Publications, **17**: 77112; https://doi.org/10.1144/GSL.SP.1984.017.01.04

Taylor, S.R., McLennan, S.M., 1995. The geochemical evolution of the continental crust. Reviews of Geophysics, **33**: 241–265; https://doi.org/10.1029/95RG00262

Tekin, U.K., 1999. Biostratigraphy and systematics of late Middle to Late Triassic radiolarians from the Taurus Mountains and Ankara region, Turkey. Geologisch-Paläontologische Mitteilungen Innsbruck, **5**: 1–297.

Tekin, U.K., Göncüoğlu, M.C., 2007. Discovery of oldest (late Ladinian to middle Carnian) radiolarian assemblages from the Bornova Flysch Zone in western Turkey: implications for the evolution of the Neotethyan Izmir-Ankara Ocean. Ofioliti, **32**: 131–150; https://doi.org/10.4454/ofioliti.v32i2.353

Tekin, U.K., Sönmez, I., 2010. Late Ladinian radiolarians from the Tahtalıdağ nappe of the Antalya nappes, SW Turkey: remarks on the late Middle and Late Triassic evolution of the Tahtalıdağ nappe. Acta Geologica Polonica, **60**: 199–217.

Tekin, U.K., Tuncer, A., 2024. Dating of sedimentary units of Karakaya Complex exposed in the near south and northeast of Ankara city centre (central Anatolia) based on radiolarian and foraminiferal fauna, interpretation of geochemistry, petrography and geodynamic evolution of volcanic/volcanosedimentary units (in Turkish with English summary). Report for Hacettepe University Scientific Research Coor. Unit, Report Number: FHD-2022-20129.

Tekin, U.K., Göncüoğlu, M.C., Pandolfi, L., Marroni, M., 2012. Middle-Late Triassic radiolarian cherts from the Arkotdağ mélange in northern Turkey: implications for the life span of the northern Neotethyan branch. Geodinamica Acta, **25**: 305–319; https://doi.org/10.1080/09853111.2013.859345

Tekin, U.K., Okuyucu, C., Sayit, K., Bedi, Y., Noble, P.J., Krystyn, L., Göncüoğlu, M.C., 2019. Integrated Radiolaria, benthic Foraminifera and conodont biochronology of the pelagic Permian blocks/tectonic slices and geochemistry of associated volcanic rocks from the Mersin Mélange, southern Turkey: Implications for the Permian evolution of the northern Neotethys. Island Arc, **28**, e12286:1–36; https://doi.org/10.1111/iar.12286

Tekin, U.K., Sarı, B., Tuncer, A., Sayit, K., Okuyucu, C., Güzgün, Ç., 2024. Radiolarian and planktonic foraminiferal biochronology of the Soğukçam Limestone Group, Elmadağ Olistostrome, and Unaz Formation (Ankara region, central Türkiye): insights into the Cretaceous evolution of the Sakarya Continent and overlying units. Carnets de Geologie, **24**: 187–263; https://doi.org/10.2110/carnets.2024.2413

Tekin, U.K., Okuyucu, C., Tuncer, A., Akbaţ, M., Sayit, K., 2025. Upper Cretaceous foreland flysch deposits from the Neotethyan Intra-Pontide Ocean: geological and palaeontological evidence from the Elmadağ Olistostrome of Ankara, central Türkiye. Lethaia, **58**: 1–30; https://doi.org/10.18261/let.58.1.7

Trifonova, E., Ivanova, D., 2001. Foraminiferal assemblages and zonation across the Lower-Middle Triassic boundary in Bulgaria. Geologica Balcanica, **31**: 49–58; https://doi.org/10.52321/GeolBalc.31.3-4.49

Tüysüz, O., 2018. Cretaceous geological evolution of the Pontides. Geological Society Special Publications, **464**: 69–94; https://doi.org/10.1144/SP464.9

Ueno, K., 1989. Carboniferous and Lower Permian foraminiferal biostratigraphy in the Akiyoshi Limestone Group-studies of the Upper Paleozoic foraminifers in the Akiyoshi Limestone Group, southwest Japan, Part 1 (in Japanese). Bulletin of the Akiyoshi-dai Science Museum, **24**: 1–40.

Ueno, K., Miyahigashi, A., Kamata, Y., Kato, M., Charoentitirat, T., Limruk, S., 2012. Geotectonic implications of Permian and Triassic carbonate successions in the Central Plain of Thailand. Journal of Asian Earth Sciences, **61**: 33–50; https://doi.org/10.1016/j.jseaes.2012.04.015

Ueno, K., Ha, T.T.N., Iryu, Y., 2019. Foraminiferal biochronology of the Triassic Hoang Mai formation, central Vietnam. Journal of Foraminiferal Research, **49**: 339–354; https://doi.org/10.2113/gsjfr.49.3.339

Ünal, E., Altıner, D., Yılmaz, I.Ö., Özkan-Altıner, S., 2003. Cyclic sedimentation across the Permian-Triassic boundary (central Taurides, Turkey). Rivista Italiana di Paleontologia e Stratigrafia, **109**: 359–376; https://doi.org/10.13130/2039-4942/5511

Vachard, D., 2016. Macroevolution and biostratigraphy of Palaeozoic Foraminifers: stratigraphy and timescales. First Edition, **1**: 257–323; https://doi.org/10.1016/bs.sats.2016.10.005

Vachard, D., Oviedo, A., Flores de Dios, A., Malpica, R., Brunner, P., Guerrero, M., Buitron, B.E., 1993. Barranca de Olinala (Guerrero): une coupe de référence pour le Permien du Mexique central; étude préliminaire. Annales de la Société Géologique du Nord, **2**: 153–160.

Vachard, D., Martini, R., Rettori, R., Zaninetti, L., 1994. Nouvelle classification de foraminifères endothyroïdes du Trias. Geobios, **27**: 543–557; https://doi.org/10.1016/S0016-6995(94)80249-1

Vachard, D., Haig, D.W., Mory, A., 2014. Lower Carboniferous (middle Visean) foraminifers and algae from an interior sea, southern Carnarvon Basin, Australia. Geobios, **47**: 57–74; https://doi.org/10.1016/j.geobios.2013.10.005

Vachard, D., Cózar, P., Aretz, M., Izart, A., 2016. Late Viséan–early Serpukhovian cyanobacteria and algae from the Montagne Noire (France); taxonomy and biostratigraphy. Bulletin of Geosciences, **91**: 433–466; https://doi.org/10.3140/bull.geosci.1613

Varol, E., Tekin, U.K., Temel, A., 2007. Age and geochemistry of middle to late Carnian basalts from the Alakırçay Nappe (Antalya Nappes, SW Turkey): implications for the evolution of southern branch of Neotethys. Ofioliti, **32**: 163–176; https://doi.org/10.4454/ofioliti.v32i2.355

Velledits, F., Péró, C., Blau, J., Senowbari-Daryan, B., Kovács, D., Piros, O., Pocsai, T., Szúgyi-Simon, H., Dumitrica, P., Palfy, J., 2011. The oldest Triassic platform margin reef from the Alpine-Carpathian region (Aggtelek, NE Hungary): platform evolution, reefal biota and biostratigraphic framework. Rivista Italiana di Paleontologia e Stratigrafia, **117:** 221–268; https://doi.org/10.13130/2039-4942/5973

Wang, E., 1982. Carboniferous and Permian foraminifera of Xizang. Palaeontology of Xizang, The series of scientific expeditions to the Qinghai-Xizang Plateau. Book IV: 1–32.

Wilson, M., Guiraud, R., 1998. Late Permian to recent magmatic activity on the African-Arabian margin of Tethys. Geological Society Special Publications, **132**: 231–263; https://doi.org/10.1144/GSL.SP.1998.132.01.14

Winchester, J.A., Floyd, P.A., 1977. Geochemical discrimination of different magma series and their differentiation products using immobile elements. Chemical Geology, **20**: 325–343; https://doi.org/10.1016/0009-2541(77)90057-2

Workman, R.K., Hart, S.R., 2005. Major and trace element composition of the depleted MORB mantle (DMM). Earth and Planetary Science Letters, **231**: 53–72; https://doi.org/10.1016/j.epsl.2004.12.005

Zaninetti, L., 1976. Les foraminifères du Trias. Essai de synthèse et corrélation entre les domains mésogéens européen et asiatique. Rivista Italiana di Paleontologia e Stratigrafia, **82**: 1–258.

Zaninetti, L., Brönnimann, P., Baud, A., 1972. Microfaciès particuliers et Foraminifères nouveaux de l'Anisien supérieur de la coupe du Rothorn (Préalpes médianes rigides, Diemtigtal, Suisse). Mitteilungen der Gesellschaft der Geologie- und Bergbaustudenten in Wien, **21**: 465–498.